cells after size fractionation of PA-labeled oligosaccharides [3,7]. Alternatively, fractionated oligosaccharides can be directly analyzed in conjunction with electrospray ionization mass spectrometry (ESI–MS), where *m/z* and GU can be obtained simultaneously. In any case, this reversed-phase HPLC is a powerful method for identification of free glycan structures (especially isomers) recovered from the cytosol of animal cells, where derivatives of Gn1-type, high-mannose-type glycans were predominant, whereas Gn2 glycans can be increased under certain conditions [12,13].

Acknowledgments

We thank the members of the Taniguchi Laboratory (Osaka University) and Dr. Akihiro Kondo (Osaka University) for valuable discussions. This study was supported in part by the COE (Center of Excellence) Program and Grants-in-Aid for Exploratory Research (18657034) from the Ministry of Education, Culture, Sports, Science, and Technology of Japan and the Osaka Cancer Foundation to T.S.

References

[1] S. Hase, T. Ikenaka, Y. Matsushima, Structure analyses of oligosaccharides by tagging of the reducing end sugars with a fluorescent compound, Biochem. Biophys. Res. Commun. 85 (1978) 257–263.
[2] S. Hase, T. Ikenaka, Y. Matsushima, A highly sensitive method for analyses of sugar moieties of glycoproteins by fluorescence labeling, J. Biochem. 90 (1981) 407–414.
[3] N. Tomiya, J. Awaya, M. Kurono, S. Endo, Y. Arata, N. Takahashi, Analyses of N-linked oligosaccharides using a two-dimensional mapping technique, Anal. Biochem. 171 (1988) 73–90.
[4] N. Takahashi, H. Nakagawa, K. Fujikawa, Y. Kawamura, N. Tomiya, Three-dimensional elution mapping of pyridylaminated N-linked neutral and sialyl oligosaccharides, Anal. Biochem. 226 (1995) 139–146.
[5] G.R. Guile, P.M. Rudd, D.R. Wing, S.B. Prime, R.A. Dwek, A rapid high-resolution high-performance liquid chromatographic method for separating glycan mixtures and analyzing oligosaccharide profiles, Anal. Biochem. 240 (1996) 210–226.
[6] K. Yanagida, S. Natsuka, S. Hase, Structural diversity of cytosolic free oligosaccharides in the human hepatoma cell line, HepG2, Glycobiology 16 (2006) 294–304.
[7] S. Hase, High-performance liquid chromatography of pyridylaminated saccharides, Methods Enzymol. 230 (1994) 225–237.
[8] S.E. Moore, R.G. Spiro, Intracellular compartmentalization and degradation of free polymannose oligosaccharides released during glycoprotein biosynthesis, J. Biol. Chem. 269 (1994) 12715–12721.
[9] S.E. Moore, C. Bauvy, P. Codogno, Endoplasmic reticulum-to-cytosol transport of free polymannose oligosaccharides in permeabilized HepG2 cells, EMBO J. 14 (1995) 6034–6042.
[10] K. Iwai, T. Mega, S. Hase, Detection of $Man_5GlcNAc$ and related free oligomannosides in the cytosol fraction of hen oviduct, J. Biochem. 125 (1999) 70–74.
[11] S. Ohashi, K. Iwai, T. Mega, S. Hase, Quantitation and isomeric structure analysis of free oligosaccharides present in the cytosol fraction of mouse liver: Detection of a free disialobiantennary oligosaccharide and glucosylated oligomannosides, J. Biochem. 126 (1999) 852–858.
[12] H.R. Mellor, D.C. Neville, D.J. Harvey, F.M. Platt, R.A. Dwek, T.D. Butters, Cellular effects of deoxynojirimycin analogues: Inhibition of N-linked oligosaccharide processing and generation of free glucosylated oligosaccharides, Biochem. J. 381 (2004) 867–875.
[13] T. Kato, K. Kitamura, M. Maeda, Y. Kimura, T. Katayama, H. Ashida, K. Yamamoto, Free oligosaccharides in the cytosol of *Caenorhabditis elegans* are generated through endoplasmic reticulum-golgi trafficking, J. Biol. Chem. 282 (2007) 22080–22088.
[14] D.S. Alonzi, D.C. Neville, R.H. Lachmann, R.A. Dwek, T.D. Butters, Glucosylated free oligosaccharides are biomarkers of endoplasmic-reticulum -glucosidase inhibition, Biochem. J. 409 (2008) 571–580.
[15] S. Hase, S. Natsuka, H. Oku, T. Ikenaka, Identification method for twelve oligomannose-type sugar chains thought to be processing intermediates of glycoproteins, Anal. Biochem. 167 (1987) 321–326.
[16] S. Hase, T. Ikenaka, Estimation of elution times on reverse-phase high-performance liquid chromatography of pyridylamino derivatives of sugar chains from glycoproteins, Anal. Biochem. 184 (1990) 135–138.
[17] Y.C. Lee, B.I. Lee, N. Tomiya, N. Takahashi, Parameterization of contribution of sugar units to elution volumes in reverse-phase HPLC of 2-pyridylaminated oligosaccharides, Anal. Biochem. 188 (1990) 259–266.
[18] K. Yanagida, H. Ogawa, K. Omichi, S. Hase, Introduction of a new scale into reversed-phase high-performance liquid chromatography of pyridylamino sugar chains for structural assignment, J. Chromatogr. A 800 (1998) 187–198.
[19] T. Suzuki, I. Hara, M. Nakano, M. Shigeta, T. Nakagawa, A. Kondo, Y. Funakoshi, N. Taniguchi, Man2C1, an -mannosidase, is involved in the trimming of free oligosaccharides in the cytosol, Biochem. J. 400 (2006) 33–41.
[20] I. Matsuo, M. Totani, A. Tatami, Y. Ito, Comprehensive synthesis of ER related high-mannose-type sugar chains by convergent strategy, Tetrahedron 62 (2006) 8262–8277.
[21] D. Fu, L. Chen, R.A. O'Neill, A detailed structural characterization of ribonuclease B oligosaccharides by ^1H NMR spectroscopy and mass spectrometry, Carbohydr. Res. 261 (1994) 173–186.
[22] I. Chantret, S.E. Moore, Free oligosaccharide regulation during mammalian protein N-glycosylation, Glycobiology 18 (2008) 210–224.
[23] T. Suzuki, Y. Funakoshi, Free N-linked oligosaccharide chains: formation and degradation, Glycoconj. J. 23 (2006) 291–302.
[24] T. Suzuki, Cytoplasmic peptide:*N*-glycanase and catabolic pathway for free *N*-glycans in the cytosol, Semin. Cell Dev. Biol. 18 (2007) 762–769.
[25] T. Suzuki, A. Seko, K. Kitajima, Y. Inoue, S. Inoue, Purification and enzymatic properties of peptide:*N*-glycanase from C3H mouse-derived L-929 fibroblast cells: Possible widespread occurrence of post-translational remodification of proteins by N-deglycosylation, J. Biol. Chem. 269 (1994) 17611–17618.
[26] T. Suzuki, H. Park, N.M. Hollingsworth, R. Sternglanz, W.J. Lennarz, *PNG1*, a yeast gene encoding a highly conserved peptide:*N*-glycanase, J. Cell Biol. 149 (2000) 1039–1052.
[27] T. Suzuki, H. Park, W.J. Lennarz, Cytoplasmic peptide:*N*-glycanase (PNGase) in eukaryotic cells: occurrence, primary structure, and potential functions, FASEB J. 16 (2002) 635–641.
[28] T. Kato, K. Hatanaka, T. Mega, S. Hase, Purification and characterization of endo-N-acetylglucosaminidase from hen oviduct, J. Biochem. 122 (1997) 1167–1173.
[29] T. Suzuki, K. Yano, S. Sugimoto, K. Kitajima, W.J. Lennarz, S. Inoue, Y. Inoue, Y. Emori, *Endo-N*-acetylglucosaminidase, an enzyme involved in processing of free oligosaccharides in the cytosol, Proc. Natl. Acad. Sci. USA 99 (2002) 9691–9696.
[30] R. Cacan, C. Dengremont, O. Labiau, D. Kmiecik, A.M. Mir, A. Verbert, Occurrence of a cytosolic neutral chitobiase activity involved in oligomannoside degradation: a study with Madin–Darby bovine kidney (MDBK) cells, Biochem. J. 313 (1996) 597–602.
[31] H. Oku, S. Hase, T. Ikenaka, Purification and characterization of neutral -mannosidase that is activated by Co^{2+} from Japanese quail oviduct, J. Biochem. 110 (1991) 29–34.
[32] M. Yamagishi, T. Ishimizu, S. Natsuka, S. Hase, Co(II)-regulated substrate specificity of cytosolic -mannosidase, J. Biochem. 132 (2002) 253–256.
[33] S.E. Moore, Oligosaccharide transport: pumping waste from the ER into lysosomes, Trends Cell Biol. 9 (1999) 441–446.

Biochemical and Biophysical Research Communications 376 (2008) 605–610

Contents lists available at ScienceDirect

Biochemical and Biophysical Research Communications

journal homepage: www.elsevier.com/locate/ybbrc

Cytoplasmic and serum galectin-3 in diagnosis of thyroid malignancies

Hidenori Inohara [a,*], Tatsuya Segawa [b], Akira Miyauchi [c], Tadashi Yoshii [a], Susumu Nakahara [a], Avraham Raz [d], Masahiro Maeda [b], Eiji Miyoshi [e], Noriaki Kinoshita [b], Hiroshi Yoshida [c], Masashi Furukawa [a], Yukinori Takenaka [a], Yuki Takamura [c], Yasuhiro Ito [c], Naoyuki Taniguchi [f]

[a] Department of Otolaryngology, Osaka University School of Medicine, 2-2 Yamadaoka, Suita, Osaka 565-0871, Japan
[b] Immuno-Biological Laboratories (IBL) Co., Ltd., Gunma, Japan
[c] Kuma Hospital, Hyogo, Japan
[d] Tumor Progression and Metastasis Program, Karmanos Cancer Institute, Michigan, USA
[e] Department of Molecular Biochemistry and Clinical Investigation, Osaka University School of Medicine, Osaka, Japan
[f] Department of Disease Glycomics (Seikagaku Corporation), Research Institute for Microbial Diseases, Osaka, Japan

ARTICLE INFO

Article history:
Received 31 August 2008
Available online 20 September 2008

Keywords:
Enzyme-linked immunosorbent assay
Galectin-3
Thyroid
Carcinoma

ABSTRACT

In order to address whether galectin-3 in the sera and fine needle aspirates serve as a diagnostic marker distinguishing between benign and malignant thyroid nodules, we developed an enzyme-linked immunosorbent assay. We quantified galectin-3 in fine needle aspirates from a series of 118 patients with thyroid nodules and serum galectin-3 from another series of 46 patients, which were compared with final histology after thyroidectomy. Relative galectin-3 value (ng/mg), defined as galectin-3 concentration (ng/ml) divided by total protein concentration (mg/ml) in fine needle aspirates, was significantly higher in papillary carcinoma than in the other thyroid entities. There was no significant difference in serum galectin-3 level among patients with thyroid nodules and healthy individuals. Accordingly, relative galectin-3 value allows a definitive diagnosis of papillary carcinoma independent of cellular morphology, whereas serum galectin-3 does not serve as a marker for papillary carcinoma.

Galectin-3, a β-galactoside-binding lectin, is presumed to be involved in carcinogenesis. Subcellular distribution of galectin-3 is predominantly in the cytoplasm [1], and cytoplasmic galectin-3 expression is increased in a diversity of human malignancies [2–4]. In particular, almost all well differentiated thyroid carcinomas express cytoplasmic galectin-3, whereas normal thyroid tissue and most benign thyroid lesions do not [2,3]. On the other hand, serum galectin-3 is less well examined, although galectin-3 is secreted [1].

Fine needle aspiration (FNA) cytology is a diagnostic procedure of first choice for the evaluation of patients with thyroid nodules [5]. Since the diagnosis of follicular carcinoma is defined by the presence of capsular or vascular invasion [6], FNA cytology is unable to differentiate follicular carcinoma from its benign counterpart. Many patients with follicular thyroid nodules are referred for thyroidectomy without real therapeutic necessity, approximately 10% of whom have malignant nodules upon surgery [7]. Moreover, false negative cytodiagnoses commonly occur in papillary carcinoma [7]. A molecular marker for malignant thyroid nodules is necessary to eliminate potentially unnecessary surgery for benign thyroid nodules and to improve the preoperative diagnostic accuracy of thyroid malignancies. In the present study, we developed an enzyme-linked immunosorbent assay (ELISA) of galectin-3. We describe a potential feasibility of cytoplasmic and serum galectin-3 concentrations for the differential diagnosis between benign and malignant thyroid nodules.

Materials and methods

Generation of MAb. Monoclonal antibodies (MAbs) were produced by a modification of the procedure of Banno et al. [8]. Female BALB/c mice of 8-week-old age were immunized by recombinant human galectin-3 prepared as described previously [9]. The isotypes of MAbs were determined with a mouse MonoAb ID EIA Kit (Zymed Laboratories Inc., San Francisco, CA). MAbs were cleaved to Fab' fragments, which were coupled to horseradish peroxidase (HRP) according to Ishikawa et al. [10]. All mice were bred in Immuno-Biological Laboratories animal facilities and used in accordance with institutional guideline.

Two-site MAb-based ELISA. Microtiter plates with 96 wells were coated with 100 μl/well of 100 mM carbonate buffer (pH9.5) containing 10 μg/ml purified anti-galectin-3 MAb at 4 °C overnight. The plates were washed with phosphate-buffered saline (PBS), pH 7.4, containing 0.05% (v/v) Tween 20 (PBS-T) and blocked with 200 μl/well of 1% (w/v) bovine serum albumin (BSA) in PBS

* Corresponding author. Fax: +81 6 6879 3959.
E-mail address: hinohara@ent.med.osaka-u.ac.jp (H. Inohara).

0006-291X/$ - see front matter © 2008 Elsevier Inc. All rights reserved.
doi:10.1016/j.bbrc.2008.09.041

containing 0.05% NaN_3 for 1 h at room temperature. Following washes with PBS-T, 100 μl of samples or purified recombinant galectin-3 as a standard, serially diluted in 1% BSA in PBS-T, were added in duplicate and incubated at 37 °C for 1 h. After washing, 100 μl of 0.2 μg/ml HRP-conjugated anti-galectin-3 MAb was added to each well and incubated for 30 min at 4 °C. Following further washing, 100 μl of freshly prepared tetramethyl benzidine solution was added to each well as a substrate and incubated in the dark for 30 min at room temperature. The reaction was terminated by the addition of 100 μl of 1 N H_2SO_4. The absorbance at 450 nm was measured in an ELISA reader (Bio-Rad, Hercules, CA).

Construction and expression of galectin-3 fusion plasmids. Four forms of truncated galectin-3 were produced as glutathione-*S*-transferase (GST) fusion proteins. cDNAs encoding amino acids (aa) 1–64 (Region #1), aa1–129 (Region #2), aa120–250 (Region #3), and aa184–250 (Region #4) were amplified by PCR using full length galectin-3 cDNA as a template. Combinations of the sense and antisense primers are as follows: Fw1 (5′-ACGGATCCAA AATGGCAGACAATTTTTCGC-3′)-Rv1 (5′-CCCTCGAGTTAAGGGTAGG CGCCTGGAGGT-3′), Fw1-Rv2 (5′-GTCTCGAGTTAGCGAGGCACCAC TCCCCCA-3′), Fw2 (5′-CTGAATTCCTGCCTTTGCCTGGGGGAGTGG-3′)-Rv3 (5′-CTCTCGAGTTATATCATGGTATATGAAGCA-3′), and Fw3 (5′-GAGAATTCGAAAGACAGTCGGTTTTCCCAT-3′)-Rv3. Full length galectin-3 cDNA was also amplified with Fw1 and Rv3. The PCR fragments were digested with BamHI and XhoI, ligated into pGEX-4T-1 vector (Amersham Biosciences, Piscataway, NJ), and transformed into *Escherichia coli* JM109 cells (Promega, Madison, WI). These five fusion proteins were expressed with IPTG induction (Sigma Chemical, St. Louis, MO) and purified by affinity chromatography using Glutathione–Sepharose 4B column (Amersham Biosciences).

Immunoblotting. Monolayer cultures of human thyroid papillary carcinoma cell line NPA and human fetal thyroid follicular cell line TAD-2 were harvested in ice-cold TNE buffer (10 mM Tris, pH 8.0, 1% NP-40, 150 mM NaCl, 1 mM EDTA). Ten micrograms of aliquots of the cell lysates was subjected to sodium dodecyl sulfate (SDS)–polyacrylamide gel electrophoresis (PAGE) on 12.5% gels under reducing conditions. After electrophoresis, the proteins were transferred to polyvinylidene difluoride (PVDF) membranes, which were quenched overnight at 4 °C. The blots were probed with anti-galectin-3 MAbs at a concentration of 1 μg/ml for 1 h, followed by treatment with HRP-conjugated rabbit anti-mouse IgG (Zymed) for 1 h. The blots were then processed for exposure with Enhanced Chemiluminescence (ECL Western blotting detection reagents; Amersham). Alternatively, the blots were probed with anti-galectin-3 MAb M3/38 produced by TIB166 hybridoma (American Type Culture Collection, Rockville, MD) and HRP-conjugated rabbit anti-rat IgG secondary antibody (Zymed). In addition, 10 μg aliquots of purified GST-fused proteins of galectin-3 were resolved by 12.5% reducing SDS–PAGE and transferred to PVDF membranes, which were probed with anti-galectin-3 MAbs or anti-GST antibody (Amersham), and processed as described above. In some experiments, fusion proteins were treated with thrombin to remove GST, and fractionated by 12.5% reducing SDS–PAGE for immunoblotting.

Patients and samples. FNA with a 22-gauge needle attached to a 10-ml syringe was performed preoperatively on a series of 118 patients with thyroid nodules. The aspirates were subjected to conventional cytology and ELISA of galectin-3. Each fine needle aspirate was rinsed with 500 μL of ice-cold TNE buffer and stored at −80 °C. All of the patients underwent thyroidectomy at Kuma Hospital in 2003, and surgically excised lesions were subjected to immunohistochemistry of galectin-3. Histopathologically the lesions consisted of 42 papillary carcinomas, 16 follicular carcinomas, 26 follicular adenomas, and 34 adenomatous goiters. Blood samples were obtained from another series of 46 patients before and 3–4 weeks after thyroidectomy at Kuma Hospital in 2002. Histopathologically the lesions consisted of 10 papillary carcinomas, 6 follicular carcinomas, 10 follicular adenomas, and 20 adenomatous goiters. The sera were stored at −80 °C until assay. Sera were also obtained from 20 healthy volunteers. Informed consent was obtained from each subject with the approval of the Institutional Review Board.

ELISA of human samples. Cell suspensions of the aspirates were gently rotated for 30 min at 4 °C and centrifuged at 12,000g for 30 min at 4 °C to remove nuclear pellet. Cell lysates and sera were serially diluted with PBS-T containing 1% BSA, and subjected to an ELISA of galectin-3 as described above. Simultaneously, total protein concentration of the cell lysate was determined using Lowry's method [11]. A relative galectin-3 value (ng/mg) was calculated by dividing galectin-3 concentration (ng/ml) by total protein concentration (mg/ml).

Immunohistochemistry. Immunohistochemistry of galectin-3 was performed by means of anti-galectin-3 MAb M3/38 and a biotin-free detection system (Histofine Simple Stain MAX PO; Nichirei, Tokyo, Japan) as described previously [12]. The distribution of cytoplasmic immunoreactivity was evaluated as follows: negative staining = 0; focal to moderate staining = 1+, when less than 40% of follicular cells were positive; diffuse staining = 2+, when greater than or equal to 40% of follicular cells were positive.

Statistical analysis. The utility of relative galectin-3 value to identify papillary carcinoma was evaluated by constructing a receiver-operating characteristic (ROC) curve. The cut-off value was defined as that which was closest to a crossing point between the ROC curve and a diagonal line representing an equality of sensitivity and specificity. The determination of 95% confidence intervals using Clopper–Pearson method was employed for statistical analysis between diagnostic modalities in terms of the diagnostic accuracy of papillary carcinoma. The difference in relative galectin-3 values between histopathological entities was analyzed by Steel Dwass test. Spearman rank coefficient was calculated to test the degree of linear association between relative galectin-3 value and immunohistochemical galectin-3 staining intensity. Serum galectin-3 level from independent groups was compared by Kruskall–Wallis test. The difference in serum galectin-3 level between pre- and post-thyroidectomy was analyzed by Wilcoxon signed rank test. A difference with $P < 0.05$ was considered significant.

Results

Characterization of anti-galectin-3 MAb

Five clones of hybridomas producing anti-galectin-3 MAbs were obtained, and designated as 11A4, 19E2, 50A3, 74E2, and 87B5. As shown in Fig. 1A, all MAbs detected a major band migrating at a molecular weight (MW) of 31 kDa in NPA cells, rich in endogenous galectin-3 [1]. Minor bands with smaller MWs were also identified, which were probably degenerated products of galectin-3. Galectin-3 is a substrate for matrix metalloproteineses-2 and -9 [13]. In contrast, all MAbs, except 11A4, detected a faint single band migrating at a MW of 31 kDa in TAD-2 cells, poor in endogenous galectin-3 [1], while 11A4 addressed a couple of non-specific bands with higher MWs. A well characterized anti-galectin-3 MAb M3/38 also recognized a band of a MW of 31 kDa. M3/38 dose not detect degenerated products of galectin-3 [13]. The isotypes of the MAbs were determined to be IgG1 (11A4, 19E2, and 50A3) and IgG2a (74E2 and 87B5).

Establishment of ELISA of galectin-3

We developed five different combinations of the MAbs for ELISA, which were evaluated in their ability to quantify galectin-3

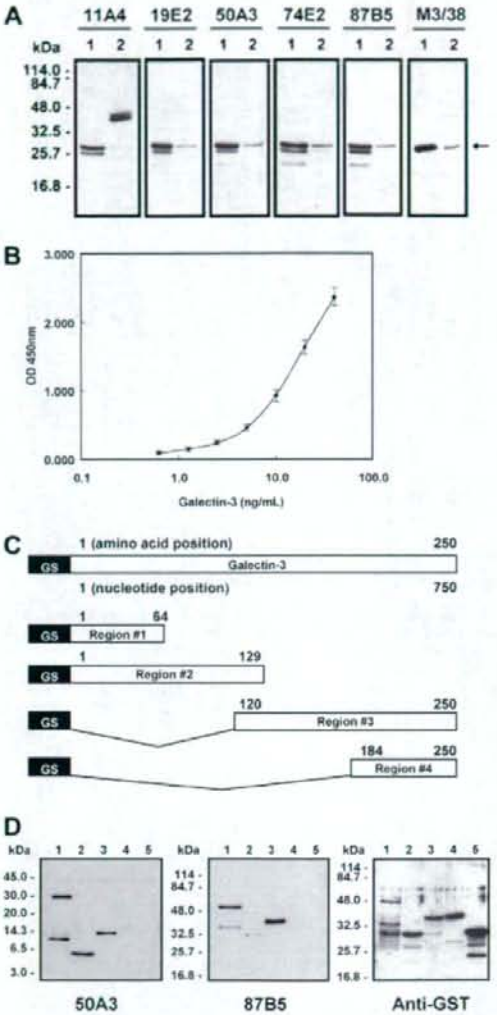

Fig. 1. Establishment of ELISA of galectin-3 and epitope mapping of anti-galectin-3 MAbs. (A) Western blot analysis by anti-galectin-3 MAbs. Lanes 1 and 2 represent NPA and TAD-2, respectively. (B) Standard dose–response curve for ELISA of galectin-3 using 50A3 (catcher) and HRP-conjugated 87B5 (detector). The bars represent SD in quadlicates. (C) Schematic of the relation of various partial sequence constructs to full-length galectin-3. The numbers above and at the ends of each construct correspond to the full-length galectin-3 cDNA and denote the first and last amino acid included in the respective fragments. (D) Epitope mapping of 50A3 and 87B5 by Western blotting. Lanes 1, 2, 3, 4, and 5 represent full-length galectin-3 protein, Regions #1, #2, #3, and #4, respectively. For Western blotting with 50A3, the lysates were digested with thrombin to dissociate galectin-3 fragments from GST because 50A3 non-specifically cross-reacts with the GST fusion protein.

expressed by NPA and TAD-2 cells. Table 1 shows galectin-3 concentrations (ng/ml) of cell lysates prepared from NPA and TAD-2 at 5×10^4 cells/mL. Although the combinations of 50A3 and 87B5, as well as 87B5 and 11A4 as catcher and detector, respectively, matched well with the immunoblotting result, the combination of 50A3 and 87B5 was selected for further study because 11A4 showed non-specific binding on immunoblotting

Table 1
Sandwich ELISA according to combinations of different MAbs

Catcher MAb	Detector MAb	Galectin-3 (ng/ml/5 × 10^4 cells)	
		NPA	TAD-2
11A4	19E2	1.5	1.1
19E2	87B5	1.7	1.3
50A3	87B5	181.9	15.7
74E2	11A4	16.8	6.1
87B5	11A4	104.5	10.9

(Fig. 1A). The standard dose–response curve of the ELISA with 50A3 and 87B5 is shown in Fig. 1B over the range of 0.624 and 40 ng/ml. To evaluate the intra- and interassay variations, two standard curves per day on 4 consecutive days were tested. The intra- and interassay coefficient variations were acceptable (<15%) (data not shown). Neither repeated freezing and thawing of sample nor presence or absence of protease inhibitors in sample buffer yielded a significant difference (data not shown).

Epitope mapping

To address the epitopes recognized by 50A3 and 87B5, galectin-3 was divided into four fragments (Regions #1:aa1–64, #2:aa1–129, #3:aa120–250, and #4:aa184–250), and expressed as GST fusion proteins with MWs of about 31, 37, 38, and 31 kDa on SDS–PAGE, respectively (Fig. 1C). These GST-truncated galectin-3 fusion proteins, as well as GST-full length galectin-3 fusion protein with a MW of approximately 50 kDa were analyzed by immunoblotting (Fig. 1D). Since, 50A3 shows a non-specific reaction against GST fusion proteins (data not shown), the galectin-3 segments were recovered from GST fusion protein after treatment with thrombin and subjected to the immunoblotting analysis. The 50A3 was able to detect Regions #1 and #2 as well as intact galectin-3, while Regions #3 and #4 were not detected, indicating that the epitope recognized by 50A3 lies within the residues of aa1–64. Likewise, the 87B5 recognized intact galectin-3, Regions #1 and #2, while it failed to detect Regions #3 and #4, suggesting that the epitope recognized by 87B5 lies also within the residues of aa1–64. Yet there is another possibility that Region #1 includes only a part of the binding region for 87B5 and that the rest could be located within the residues of aa65–119, because the 87B5 recognizes Region #2 much stronger than Region #1.

Relative galectin-3 value

Fine needle aspirates, the majority of which consist of follicular cells, differ in cell number between samples. In order to neutralize the difference, galectin-3 concentration measured by ELISA was divided by total protein concentration in the aspirates, which yielded a relative galectin-3 value. Relative galectin-3 value (median, range) was 214, 2.3–1260 for papillary carcinoma, 10.1, 0.5–53.4 for follicular carcinoma, 6.0, 0.16–23.4 for follicular adenoma, and 6.1, 0.34–55.3 for adenomatous goiter (Fig. 2A). Papillary carcinoma showed significantly higher relative galectin-3 values than the follicular entities ($P < 0.0001$). There was no statistically significant difference in relative galectin-3 values among the follicular entities.

Diagnosis of papillary carcinoma

We evaluated the utility of relative galectin-3 value to diagnose papillary carcinoma. A ROC curve was drawn to determine the cut-off value distinguishing papillary carcinoma from follicular lesions, which was defined as 38.4 (Fig. 2B). The sensitivity, specificity positive predictive value, and negative predictive value of relative galectin-3 value were 88%, 92%, 86%, and 93%, respectively, while

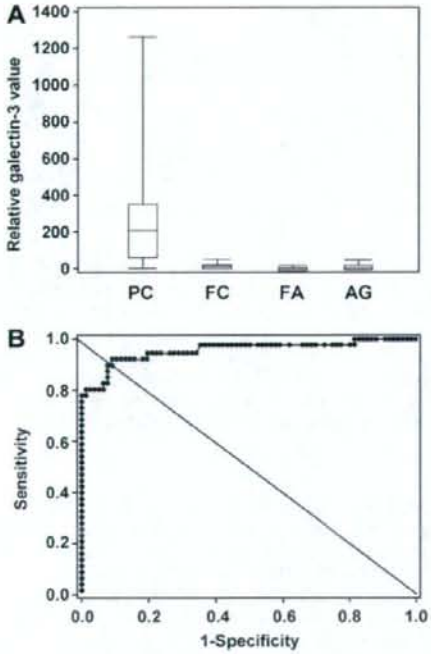

Fig. 2. Stratification of thyroid lesions by relative galectin-3 value. (A) Relative galectin-3 value in thyroid lesions. The box represents the difference between the 25th and 75th percentiles, whereas the horizontal line inside the box represents the median. Whiskers are drawn from the ends of the box to the maximum and minimum values. PC, papillary carcinoma; FC, follicular carcinoma; FA, follicular adenoma; AG, adenomatous goiter. (B) Receiver-operating characteristic curves for relative galectin-3 value in the diagnosis of papillary carcinoma. A diagonal line represents an equality of sensitivity and specificity.

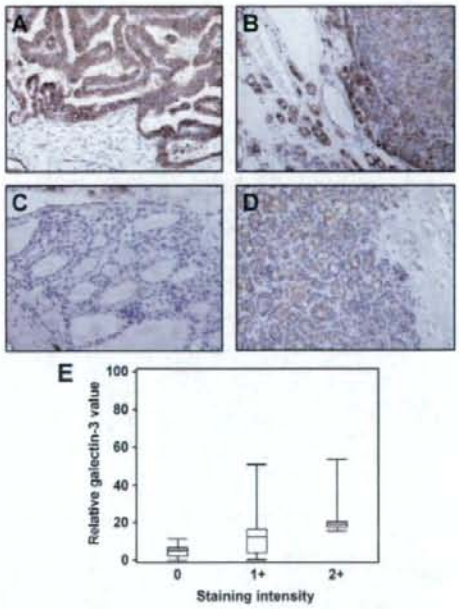

Fig. 3. Immunohistochemical analysis of galectin-3 in thyroid lesions (A–D) and relative galectin-3 value according to staining intensity of thyroid follicular tumors (E). (A) Papillary carcinoma (staining level 2+); (B) follicular carcinoma (staining level 2+); (C) follicular adenoma (staining level 0); (D) follicular adenoma (staining level 1+). (E) The box represents the difference between the 25th and 75th percentiles, whereas the horizontal line inside the box represents the median. Whiskers are drawn from the ends of the box to the maximum and minimum values.

those of cytology were 86%, 96%, 100%, and 92%, respectively. There was no significant difference in a diagnostic accuracy between the two modalities

Immunohistochemistry of galectin-3

Two of 42 papillary carcinomas were not analyzed because the specimens peeled off the slides due to excessive calcification. Fig. 3A–D shows the representative immunohistochemistry of each thyroid entity. Galectin-3, when expressed, was predominantly found in the cytoplasm of follicular cells. Papillary carcinoma generally showed more intense expression of galectin-3, as compared with follicular lesions. Galectin-3 expression was never detected in follicular cells of normal thyroid tissue adjacent to neoplastic or hyperplastic lesions. In the stroma, galectin-3 was observed in a diversity of cells, such as fibroblasts, endothelial and smooth muscle cells, and macrophages. Table 2 summarizes the immunohistochemical results.

Association between ELISA and immunohistochemistry

Since follicular lesions showed variable levels of immunohistochemical galectin-3, it was of interest to address whether relative galectin-3 value correlated with staining intensity. As depicted in Fig. 3E, relative galectin-3 value (median, range) was 5.6, 0.16–11.2 for 0 staining intensity, 12.4, 0.65–51.1 for 1+, and 19.3, 15.9–53.4 for 2+ when follicular adenomas and carcinomas were

Table 2
Immunohistochemical galectin-3 in thyroid nodules

Histology	No. of patients	Staining level			% Positive
		0 (%)	1+ (%)	2+ (%)	
Papillary carcinoma	40	0 (0)	4 (10)	36 (90)	100
Follicular carcinoma	16	6 (38)	7 (44)	3 (19)	63
Follicular adenoma	26	17 (65)	6 (23)	3 (12)	35
Adenomatous goiter	34	26 (76)	6 (18)	2 (6)	24

combined. There was a significant association between relative galectin-3 value and staining intensity (Spearman rank coefficient = 0.588, $P < 0.0001$). When adenomatous goiters were further combined, the association became less significant (Spearman rank coefficient = 0.287, $P = 0.003$).

Serum galectin-3

The level of serum galectin-3 is summarized in Table 3. There was no significant difference in serum galectin-3 level among patients with thyroid nodules and healthy individuals. After thyroidectomy, serum galectin-3 level of patients with adenomatous goiter was significantly decreased ($P = 0.002$), whereas that of patients with the other thyroid entities showed no significant change.

Discussion

Relative galectin-3 value yielded a diagnostic accuracy for papillary carcinoma, comparable to cytodiagnosis. Five of 42 papillary

Table 3
Serum galectin-3 among patients with thyroid nodules and healthy controls

Diagnosis	No.	Thyroidectomy	Serum galectin-3 (ng/ml)		
			Median	Range	*P*-value
Healthy individuals	20		1.1	0.31–2.1	
Papillary carcinoma	10	Pre	1.8	0.36–6.9	
		Post	1.8	0.84–7.1	
Follicular carcinoma	6	Pre	1.4	0.77–5.2	
		Post	1.8	0.41–6.9	
Follicular adenoma	10	Pre	1.2	0.53–4.9	
		Post	1.5	0.31–4.3	
Adenomatous goiter	20	Pre	1.6	0.31–4.1	0.002*
		Post	0.31	0.31–5.5	

* *P*-value refers to the difference between the groups of pre- and post-thyroidectomy.

carcinomas (12%) showed relative galectin-3 values less than the cut-off (false negative results), which was probably due to sampling error, because all of these cases showed diffuse expression of galectin-3 on immunohistochemistry. Only single aspirate of each thyroid nodule was subjected to the analysis of relative galectin-3 value. Noteworthy is that both of two papillary carcinomas with non-diagnostic cytological results after repeated FNA showed relative galectin-3 values higher than the cut-off. When relative galectin-3 value was combined with cytology, the sensitivity was increased up to 100%. This increment was not statistically significant because the sensitivities of the two modalities were high by themselves. There were six cases with false positive results, two and four of which were follicular carcinomas and adenomatous goiters, respectively. None of follicular adenomas showed false positive results. Among four adenomatous goiters with false positive results, two showed no expression of galectin-3 on immunohistochemistry, suggesting that contamination of galectin-3-positive inflammatory cells such as macrophages caused false positive results. It should be noted that a subset of aspirates from adenomatous goiters show moderate to abundant background macrophages [14]. Moreover, it has been reported that the presence of macrophages explains the false positive expression of galectin-3 in aspirates of adenomatous goiters [15].

Relative galectin-3 value failed to identify follicular carcinoma among follicular lesions, although relative galectin-3 value of follicular carcinoma tended to be higher than that of the other follicular entities. This is at least in part attributed to the finding that 9 of 26 follicular adenomas (35%) and 10 of 16 follicular carcinomas (63%) immunohistochemically expressed galectin-3, since there was a positive correlation between relative galectin-3 value and immunohistochemical staining intensity. This immunohistochemical results disagree with previous literature [2,3], because of the failure to show a close relationship of galectin-3 with malignant phenotype in follicular lesions. Observer variation of histopathological diagnosis may explain the discrepancy at least in part. The dissociation of relative galectin-3 value with immunohistochemical results among adenomatous goiters is explained, at least in part, by the contamination of macrophages in aspirates as described above.

Observer variation has long been a recurrent topic in the diagnosis of follicular lesions. Follicular carcinoma is subdivided into minimally and widely invasive types. Since widely invasive follicular carcinoma shows extensive invasion, pathologists have less difficulty in diagnosing the follicular lesion as malignant, and the reproducibility of diagnosis among pathologists is within acceptance [16]. In contrast, the histopathological reproducibility of minimally invasive follicular carcinoma is low because the evaluation of vascular or capsular invasion is less reproducible [16]. More explicit criteria for diagnosis of follicular lesions, minimizing the impact of observer variation, are needed to establish the relevance of galectin-3 in benign and malignant phenotypes among follicular lesions. Interestingly, Saggiorato et al. reported that galectin-3-positive follicular adenomas showed histological features suspicious of malignancy, such as hypercellularity, increased nucleus–cytoplasm ratio, and mitoses [17].

Serum galectin-3 concentration of patients with papillary carcinomas did not differ significantly from that of patients with follicular lesions and healthy individuals. Under organ culture, medium conditioned by papillary carcinoma tissue contained a 7-fold higher concentration of galectin-3 than that conditioned by normal adjacent thyroid tissue (data not shown). It seems likely that papillary carcinoma secretes galectin-3 in the circulation under certain stimuli. On the other hand, only patients with adenomatous goiter showed a decreased level of serum galectin-3 after thyroidectomy, suggesting that the source producing serum galectin-3 may vary among thyroid entities. Infiltrating inflammatory cells expressing galectin-3 are responsible, at least in part, for serum galectin-3 in patients with adenomatous goiters. Since a diversity of cells involved in immune system secrete galectin-3 [18], immune system seems likely to be concerned with serum galectin-3.

In conclusion, we have developed an ELISA of galectin-3 which allows a quick and quantitative measurement of galectin-3. Relative galectin-3 value is useful for the definitive diagnosis of papillary carcinoma independent of cellular morphology, and complements FNA cytology, although serum galectin-3 does not serve as a marker for papillary carcinoma.

Acknowledgments

This work was supported in part by a grant from the Senri Life Science Foundation (to H.I.). We are grateful to Seishi Yamamoto for statistical analysis and Rebecca Honjo for editing the manuscript.

References

[1] S.H. Barondes, D.N. Cooper, M.A. Gitt, H. Leffler, Galectins: structure and function of a large family of animal lectins, J. Biol. Chem. 269 (1994) 20807–20810.
[2] H. Inohara, Y. Honjo, T. Yoshii, et al., Expression of galectin-3 in fine-needle aspirates as a diagnostic marker differentiating benign from malignant thyroid neoplasms, Cancer 85 (1999) 2475–2484.
[3] A. Bartolazzi, A. Gasbarri, M. Papotti, et al., Application of an immunodiagnostic method for improving preoperative diagnosis of nodular thyroid lesions, Lancet 357 (2001) 1644–1650.
[4] H.L. Schoeppner, A. Raz, S.B. Ho, R.S. Bresalier, Expression of an endogenous galactose-binding lectin correlates with neoplastic progression in the colon, Cancer 75 (1995) 2818–2826.
[5] H. Gharib, J.R. Goellner, Fine needle aspiration biopsy of the thyroid: an appraisal, Ann. Intern. Med. 118 (1993) 282–289.
[6] C.H.R. Hedlinger, Histological typing of thyroid tumors, WHO, Geneva, 1988.
[7] C. Ravetto, L. Colombo, M.E. Dottorini, Usefulness of fine-needle aspiration in the diagnosis of thyroid carcinoma: a retrospective study in 37,895 patients, Cancer 90 (2000) 357–363.
[8] S. Banno, K. Yoshikawa, S. Nakamura, et al., Monoclonal antibody against PRAD1/cyclin D1 tains nuclei of tumor cells with translocation or amplification at BCL-1 locus, Jpn. J. Canser Res. 85 (1994) 918–926.
[9] J. Ochieng, D. Platt, L. Tait, et al., Structure–function relationship of a recombinant human galactoside-binding protein, Biochemistry 32 (1993) 4455–4460.
[10] E. Ishikawa, S. Yoshitake, M. Imagawa, A. Sumiyoshi, Preparation of monomeric Fab'-horseradish peroxidase conjugate using thiol groups in the hinge and its evaluation in enzyme immunoassay and immunohistochemical staining, Ann. NY Acad. Sci. 420 (1983) 74–89.
[11] O.H. Lowry, N.J. Rosebrough, A.L. Farr, R.J. Randall, Protein measurement with the Folin phenol reagent, J. Biol. Chem. 193 (1951) 265–275.
[12] E. Saggiorato, S. Aversa, D. Deandreis, et al., Galectin-3: presurgical marker of thyroid follicular epithelial cell-derived carcinomas, J. Endocrinol. Invest. 27 (2004) 311–317.
[13] J. Ochieng, R. Fridman, P. Nangia-Makker, et al., Galectin-3 is a novel substrate for human matrix metalloproteinases-2 and -9, Biochemistry 33 (1994) 14109–14114.
[14] H.R. Harach, S.B. Zusman, E. Saravia Day, Nodular goiter: a histo-cytological study with some emphasis on pitfalls of fine-needle aspiration cytology, Diagn. Cytopathol. 8 (1992) 409–419.

[15] N. Mateša, I. Šamija, Z. Kusić, Galectin-3 and CD44v6 positivity by RT-PCR method in fine needle aspirates of benign thyroid lesions, Cytopathology 18 (2007) 112–116.
[16] B. Franc, P. de la Sarmoniere, F. Lange, et al., Interobserver and intraobserver reproducibility in the histopathology of follicular thyroid carcinoma, Hum. Pathol. 34 (2003) 1092–1100.
[17] E. Saggiorato, S. Cappia, P. De Giuli, et al., Galectin-3 as a presurgical immunocytodiagnostic marker of minimally invasive follicular thyroid carcinoma, J. Clin. Endocrinol. Metab. 86 (2001) 5152–5158.
[18] H.Y. Chen, F.T. Liu, R.Y. Yang, Roles of galectin-3 in immune responses, Arch. Immunol. Ther. Exp. 53 (2005) 497–504.

[Cell Adhesion & Migration 2:4, 243-245; October/November/December 2008]; ©2008 Landes Bioscience

Commentary & View

Potential of N-glycan in cell adhesion and migration as either a positive or negative regulator

Jianguo Gu[1,*] and Naoyuki Taniguchi[2,3]

[1]Division of Regulatory Glycobiology; Institute of Molecular Biomembrane and Glycobiology; Tohoku Pharmaceutical University; Sendai, Miyagi, Japan; [2]Department of Disease Glycomcis; Institute for Microbial Diseases; Osaka University; Suita, Osaka, Japan; [3]Systems Glycobiology Group; Disease Glycomics Team; Advanced Science Institute; Riken, Wako, Japan

Key words: integrin, E-cadherin, GnT-III, GnT-V, N-glycosylation, glycosyltransferase

Glycosylation is one of the most abundant posttranslational modification reactions, and nearly half of all known proteins in eukaryotes are glycosylated. In fact, changes in oligosaccharide structure (glycan) are associated with many physiological and pathological events, including cell adhesion, migration, cell growth, cell differentiation and tumor invasion. Glycosylation reactions are catalyzed by the action of glycosyltransferases, which add sugar chains to various complex carbohydrates such as glycoproteins, glycolipids and proteoglycans. Functional glycomics, which uses sugar remodeling by glycosyltransferases, is a promising tool for the characterization of glycan functions. Here, we will focus on the positive and negative regulation of biological functions of integrins by the remodeling of *N*-glycans with *N*-acetylglucosaminyltransferase III (GnT-III) and *N*-acetylglucosaminyltransferase V (GnT-V), which catalyze branched N-glycan formations, bisecting GlcNAc and β1,6 GlcNAc, respectively. Typically, integrins are modified by GnT-III, which inhibits cell migration and cancer metastasis. In contrast, integrins modified by GnT-V promote cell migration and cancer invasion.

Protein glycosylation encompasses N-glycans, O-glycans and Glycosaminoglycans. N-glycans are linked to asparagine residues of proteins, which is a specific subset residing in the Asn-X-Ser/Thr motif, whereas O-glycans are attached to a subset of serines and threonines (Fig. 1).[1] An increasing body of evidence indicates that glycans in glycoproteins are involved in the regulation of cellular functions including cell-cell communication and signal transduction.[2,3] In fact, most receptors on the cell surface are *N*-glycosylated—integrins and epithelial growth factor receptors; and transforming growth factor β receptors. Here, we focus mainly on the modification of *N*-glycans of integrin α3β1 and α5β1 to address the important roles of *N*-glycans in cell adhesion and migration.

Previous studies indicate that the presence of the appropriate oligosaccharide can modulate integrin activation. When human fibroblasts were cultured in the presence of l-deoxymannojirimycin, an inhibitor of α-mannosidase II, which prevents *N*-linked oligosaccharide processing, immature α5β1 integrin appeared at the cell surface, and fibronectin (FN)-dependent adhesion was greatly reduced.[4] In addition, the treatment of purified integrin α5β1 with *N*-glycosidase F, which cleaves between the innermost GlcNAc and asparagine residues of *N*-glycans from *N*-linked glycoproteins, resulted in the blockage of α5β1 binding to FN and the inherent association of both subunits,[5] suggesting that *N*-glycosylation is essential for functional integrin α5β1. The production of glycoprotein glycans is catalyzed by various glycosyltransferases. *N*-Acetylglucosaminyltransferase III (GnT-III) transfers N-acetylglucosamine (GlcNAc) from UDP-GlcNAc to a β1, 4 mannose in *N*-glycans to form a "bisecting" GlcNAc linkage, as shown in Figure 2. Bisecting GlcNAc linkage is found in various hybrid and complex *N*-glycans. GnT-III is generally regarded as a key glycosyltransferase in *N*-glycan biosynthetic pathways. Introduction of a bisecting GlcNAc suppresses further processing and elongation of *N*-glycans catalyzed by *N*-acetylglucosaminyltransferase V (GnT-V), which is strongly associated with cancer metastasis, since GnT-V cannot utilize the bisected oligosaccharide as a substrate.[6-8] It has also been reported that GnT-V activity and β1, 6 branched *N*-glycan levels are increased in highly metastatic tumor cell lines.[9,10] When NIH3T3 cells were transformed with the oncogenic Ras gene, cell spreading on FN was greatly enhanced due to an increase in β1, 6 GlcNAc branched tri- and tetra-antennary oligosaccharides in α5β1 integrins.[9] Similarly, the characterization of N-glycans of integrin α3β1 from non-metastatic and metastatic human melanoma cell lines showed that β1, 6 GlcNAc branched structures were expressed at high levels in metastatic cells compared with non-metastatic cells.[10] Cancer metastasis was consistently, and significantly, suppressed in GnT-V knockout mice.[11]

To explore the possible mechanisms involved in increased β1, six branched *N*-glycans on cancer cells, Guo et al. found that cell migration toward FN and invasion through the matrigel were both substantially stimulated in cells in which the expression of GnT-V was induced.[12] Increased branched sugar chains inhibited the clustering of integrin α5β1 and the organization of F-actin into extended microfilaments in cells plated on FN-coated plates, which supports the hypothesis that the degree of adhesion of cells to their extracellular matrix (ECM) substrate is a critical factor in regulating the rate of cell migration, i.e., migration is maximal under conditions of intermediate levels of cell adhesion.[13] Conversely, GnT-V null mouse

*Correspondence to: Jianguo Gu; Division of Regulatory Glycobiology; Institute of Molecular Biomembrane and Glycobiology; Tohoku Pharmaceutical University; Sendai, Miyagi, 981-8558 Japan; Email: jgu@tohoku-pharm.ac.jp

Submitted: 04/28/08; Accepted: 08/05/08

Previously published online as a *Cell Adhesion & Migration* E-publication: http://www.landesbioscience.com/journals/celladhesion/article/6748

embryonic fibroblasts (MEF) displayed enhanced cell adhesion to, and spreading on, FN-coated plates with the concomitant inhibition of cell migration. The restoration of GnT-V cDNA in the null MEF reversed these abnormal characteristics, indicating the direct involvement of *N*-glycosylation events in these phenotypic changes.

In contrast to GnT-V, the overexpression of GnT-III resulted in an inhibition of α5β1 integrin-mediatedcell spreading and migration, and the phosphorylation of the focal adhesion kinase.[14] The affinity of the binding of integrin α5β1 to FN was significantly reduced as a result of the introduction of a bisecting GlcNAc to the α5 subunit. In addition, overexpression of GnT-III in highly metastatic melanoma cells reduced β1, six branching in cell-surface *N*-glycans and increased bisected *N*-glycans.[15] Therefore, GnT-III has been proposed as an antagonistic of GnT-V, thereby contributing to the suppression of cancer metastasis. In fact, the opposing effects of GnT-III and GnT-V have been observed for the same target protein, integrin α3β1.[16] GnT-V stimulates α3β1 integrin-mediated cell migration, while overexpression of GnT-III inhibits GnT-V-induced cell migration. The modification of the α3 subunit by GnT-III supersedes modification by GnT-V. As a result, GnT-III inhibits GnT-V-induced cell migration. These results strongly suggest that remodeling of glycosyltransferase-modified *N*-glycan structures either positively or negatively modulates cell adhesion and migration.

In addition, sialylation on the non-reducing terminus of *N*-glycans of α5β1 integrin plays an important role in cell adhesion. The increased sialylation of the β1 integrin subunit was correlated with a decreased adhesiveness and metastatic potential.[17-19] On the other hand, the enzymatic removal of α2, eight-linked oligosialic acids from the α5 integrin subunit inhibited cell adhesion to FN,[20] supporting the observation that the *N*-glycans of α and β integrin subunits play distinct roles in cell-ECM interactions.[21] Collectively, these findings suggest that the interaction of integrin α5β1 with FN is dependent on *N*-glycosylation and the processing status of *N*-glycans.

Although alteration of the oligosaccharide portion on integrin α5β1 could affect cis- and trans-interactions caused by GnT-III, ST6Gall and GnT-V, as described above, the molecular mechanism remains unclear. Considering integrin α5β1 contains 26 potential *N*-linked glycosylation sites (14 in the α subunit and 12 in the β subunit), the determination of those crucial *N*-glycosylation sites for its biological function is, therefore, quite important for an understanding of the underlying mechanism. We sequentially mutated either one or a combination of asparagine residues in the putative *N*-glycosylation sites of glutamine residues, and found that *N*-glycosylation on the β-propeller domain of the α5 subunit (in particular sites number 3–5) is essential for its hetero-dimer formation and its biological functions such as cell spreading and cell migration, as well as for the proper folding of the α5 subunit.[22] On the other hand, N-glycans on β1 integrin also play important roles in the regulation of its biological functions[23,24] (and our unpublished data). Very recently, we also found that GnT-III specifically modifies one of the important glycosylation sites, which results in functional regulation (unpublished data). We postulate that these important sites may participate in supramolecular complex formation on the cell surface, which controls intracellular signal transduction.

It also is worth noting that N-glycans regulate cell-ECM association as well as cell-cell adhesion. Overexpression of GnT-III slowed E-cadherin turnover, resulting in increased E-cadherin expression on the surface of B16 melanoma cells.[25] E-cadherin engagement at cell-cell contacts is known to suppress cell migration, and that effect has been best described in the context of tumorigenesis.[26] Conversely, the disruption of E-cadherin-mediated cell adhesion appears to be a central event in the transition from non-invasive to invasive carcinomas. Interestingly, we recently found that E-cadherin-mediated cell-cell interaction upregulated GnT-III expression,[27,28] suggesting that regulation of GnT-III and E-cadherin expression may exist as a positive feedback loop. Taken together, the overexpression of GnT-III inhibits cell migration by at least two mechanisms: an enhancement in cell-cell adhesion and a downregulation of cell-ECM adhesion (Fig. 2).

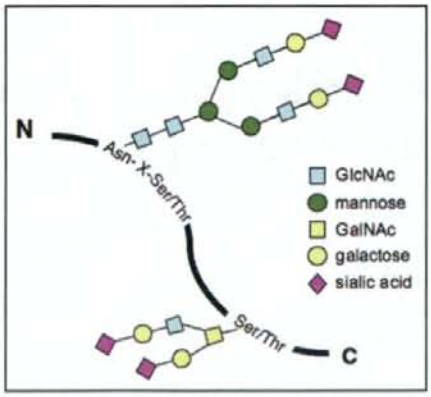

Figure 1. Two major types of protein glycosylation. N-glycans are covalently linked to asparagine (Asn) residue of proteins, specifically the Asn-X-Ser/Thr motif. In contrast, O-glycans are attached to a subset of glycosidically linked hydroxyl groups of the amino acids serine (Ser) and threonine (Thr).

Indeed, glycosylation defects in humans and their links to disease have shown that the mammalian glycome contains a significant amount of biological information.[29] The mammalian glycome repertoire is estimated to be between hundreds and thousands of glycan structures and could be larger than its proteome counterpart. Nevertheless, characterization of the biological functions of each glycan could one day make a significant contribution to the diagnosis and treatment of disease.

Acknowledgements

These works were partly supported by Core Research for Evolutional Science and Technology (CREST), the Japan Science and Technology Agency (JST) and the "Academic Frontier" Project for Private Universities from the Ministry of Education, Culture, Sports, Science and Technology of Japan, and the core to core program (JSPS). The authors are deeply indebted to the outstanding related papers which have not been cited in the present article due to limited space.

References

1. Schachter H. The joys of HexNAc. The synthesis and function of N- and O-glycan branches. Glycoconj J 2000; 17:465-83.
2. Saxon E, Bertozzi CR. Chemical and biological strategies for engineering cell surface glycosylation. Annu Rev Cell Dev Biol 2001; 17:1-23.
3. Taniguchi N, Miyoshi E, Gu J, Honke K, Matsumoto A. Decoding sugar functions by identifying target glycoproteins. Curr Opin Struct Biol 2006; 16:561-6.
4. Akiyama SK, Yamada SS, Yamada KM. Analysis of the role of glycosylation of the human fibronectin receptor. J Biol Chem 1989; 264:18011-8.

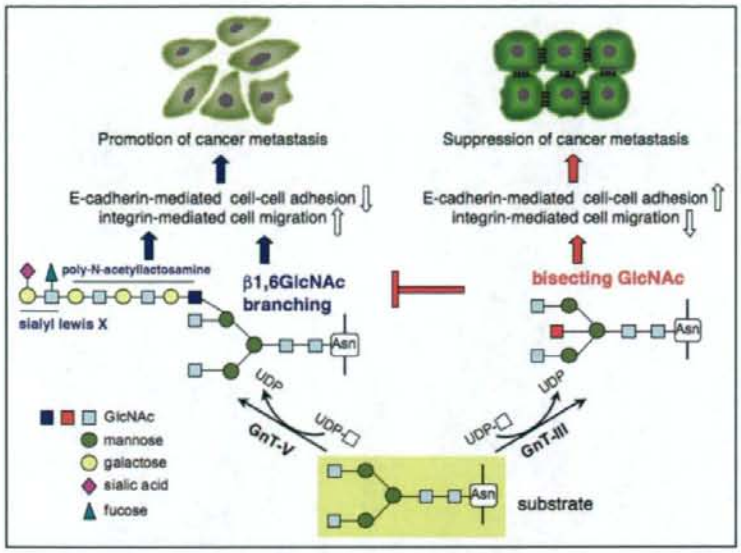

Figure 2. Glycosylation reactions catalyzed by the action of glycosyltransferase GnT-III and GnT-V. The remodeled N-glycans regulate cell adhesion and migration. Enhanced expression of GnT-V in epithelial cells results in a loss of cell-cell adhesion, increasing integrin-mediated cell migration. In contrast, overexpression of GnT-III strengthens cell-cell interaction and downregulates integrin-mediated cell migration, which may contribute to the suppression of cancer metastasis. The β1,6GlcNAc branching is preferentially modified by polylactosamine and other sugar motifs such as sialyl Lewis X, which also contribute to promotion of cancer metastasis. It is worth mentioning that GnT-III could be proposed as an antagonistic of GnT-V, since GnT-V cannot utilize the bisected oligosaccharide as a substrate.

5. Zheng M, Fang H, Hakomori S. Functional role of N-glycosylation in alpha5beta1 integrin receptor. De-N-glycosylation induces dissociation or altered association of alpha5 and beta1 subunits and concomitant loss of fibronectin binding activity. J Biol Chem 1994; 269:12325-31.
6. Gu J, Nishikawa A, Tsuruoka N, Ohno M, Yamaguchi N, Kangawa K, et al. Purification and characterization of UDP-N-acetylglucosamine: alpha-6-D-mannoside beta1-6N-acetylglucosaminyltransferase (N-acetylglucosaminyltransferase V) from a human lung cancer cell line. J Biochem (Tokyo) 1993; 113:614-9.
7. Schachter H. Biosynthetic controls that determine the branching and microheterogeneity of protein-bound oligosaccharides. Adv Exp Med Biol 1986; 205:53-85.
8. Schachter H, Narasimhan S, Gleeson P, Vella G. Control of branching during the biosynthesis of asparagine-linked oligosaccharides. Can J Biochem Cell Biol 1983; 61:1049-66.
9. Asada M, Furukawa K, Segawa K, Endo T, Kobata A. Increased expression of highly branched N-glycans at cell surface is correlated with the malignant phenotypes of mouse tumor cells. Cancer Res 1997; 57:1073-80.
10. Pochec E, Litynska A, Amoresano A, Casbarra A. Glycosylation profile of integrin alpha3-beta1 changes with melanoma progression. Biochim Biophys Acta 2003; 7:1-3.
11. Granovsky M, Fata J, Pawling J, Muller WJ, Khokha R, Dennis JW. Suppression of tumor growth and metastasis in Mgat5-deficient mice. Nat Med 2000; 6:306-12.
12. Guo HB, Lee I, Kamar M, Akiyama SK, Pierce M. Aberrant N-glycosylation of beta1 integrin causes reduced alpha5beta1 integrin clustering and stimulates cell migration. Cancer Res 2002; 62:6837-45.
13. Palecek SP, Loftus JC, Ginsberg MH, Lauffenburger DA, Horwitz AF. Integrin-ligand binding properties govern cell migration speed through cell-substratum adhesiveness. Nature 1997; 385:537-40.
14. Isaji T, Gu J, Nishiuchi R, Zhao Y, Takahashi M, Miyoshi E, et al. Introduction of bisecting GlcNAc into integrin alpha5beta1 reduces ligand binding and downregulates cell adhesion and cell migration. J Biol Chem 2004; 3:3.
15. Yoshimura M, Nishikawa A, Ihara Y, Taniguchi S, Taniguchi N. Suppression of lung metastasis of B16 mouse melanoma by N-acetylglucosaminyltransferase III gene transfection. Proc Natl Acad Sci USA 1995; 92:8754-8.
16. Zhao Y, Nakagawa T, Itoh S, Inamori K, Isaji T, Kariya Y, et al. N-acetylglucosaminyltransferase III antagonizes the effect of N-acetylglucosaminyltransferase V on alpha3beta1 integrin-mediated cell migration. J Biol Chem 2006; 281:32122-30.
17. Pretzlaff RK, Xue VW, Rowin ME. Sialidase treatment exposes the beta1-integrin active ligand binding site on HL60 cells and increases binding to fibronectin. Cell Adhes Commun 2000; 7:491-500.
18. Kawano T, Takasaki S, Tao TW, Kobata A. Altered glycosylation of beta1 integrins associated with reduced adhesiveness to fibronectin and laminin. Int J Cancer 1993; 53:91-6.
19. Dennis J, Waller C, Timpl R, Schirrmacher V. Surface sialic acid reduces attachment of metastatic tumour cells to collagen type IV and fibronectin. Nature 1982; 300:274-6.
20. Nadanaka S, Sato C, Kitajima K, Katagiri K, Irie S, Yamagata T. Occurrence of oligosialic acids on integrin alpha5 subunit and their involvement in cell adhesion to fibronectin. J Biol Chem 2001; 276:33657-64.
21. Chammas R, Veiga SS, Travassos LR, Brentani RR. Functionally distinct roles for glycosylation of alpha and beta integrin chains in cell-matrix interactions. Proc Natl Acad Sci USA 1993; 90:1795-9.
22. Isaji T, Sato Y, Zhao Y, Miyoshi E, Wada Y, Taniguchi N, Gu J. N-glycosylation of the beta-propeller domain of the integrin alpha5 subunit is essential for alpha5beta1 heterodimerization, expression on the cell surface, and its biological function. J Biol Chem 2006; 281:33258-67.
23. Zhuo Y, Chammas R, Bellis SL. Sialylation of beta1 integrins blocks cell adhesion to galectin-3 and protects cells against galectin-3-induced apoptosis. J Biol Chem 2008.
24. Seales EC, Jurado GA, Brunson BA, Wakefield JK, Frost AR, Bellis SL. Hypersialylation of beta1 integrins, observed in colon adenocarcinoma, may contribute to cancer progression by upregulating cell motility. Cancer Res 2005; 65:4645-52.
25. Yoshimura M, Ihara Y, Matsuzawa Y, Taniguchi N. Aberrant glycosylation of E-cadherin enhances cell-cell binding to suppress metastasis. J Biol Chem 1996; 271:13811-5.
26. Hirohashi S. Inactivation of the E-cadherin-mediated cell adhesion system in human cancers. Am J Pathol 1998; 153:333-9.
27. Akama R, Sato Y, Kariya Y, Isaji T, Fukuda T, Lu L, et al. N-Acetylglucosaminyltransferase III Expression Is Regulated by Cell-Cell Adhesion via the E-cadherin-catenin-actin Complex. Proteomics 2008; 8:3221-8.
28. Iijima J, Zhao Y, Isaji T, Kameyama A, Nakaya S, Wang X, et al. Cell-cell interaction-dependent regulation of N-acetylglucosaminyltransferase III and the bisected N-glycans in GE11 epithelial cells. Involvement of E-cadherin-mediated cell adhesion. J Biol Chem 2006; 281:13038-46.
29. Freeze HH. Genetic defects in the human glycome. Nat Rev Genet 2006; 7:537-51.

Immunology
The journal of cells, molecules, systems and technologies

British Society for immunology

IMMUNOLOGY ORIGINAL ARTICLE

β_2-Adrenergic receptor regulates Toll-like receptor-4-induced nuclear factor-κB activation through β-arrestin 2

Takako Kizaki,[1] Tetsuya Izawa,[2] Takuya Sakurai,[1] Shukoh Haga,[3] Naoyuki Taniguchi,[4] Hisao Tajiri,[5] Kenji Watanabe,[6] Noorbibi K. Day,[7] Kenji Toba[8] and Hideki Ohno[1]

[1]*Department of Molecular Predictive Medicine and Sport Science, Kyorin University, School of Medicine, Mitaka, Japan,* [2]*Department of Kinesiology, Graduate School of Science, Tokyo Metropolitan University, Hachioji, Japan,* [3]*Institute of Health and Sport Sciences, University of Tsukuba, Tsukuba, Japan,* [4]*Department of Biochemistry, Osaka University Medical School, Suita, Japan,* [5]*Division of Gastroenterology and Hepatology, Department of Internal Medicine, The Jikei University School of Medicine, Tokyo, Japan,* [6]*Watanabe Clinic, Shizuoka, Japan,* [7]*Department of Pediatrics, University of South Florida/All Children's Hospital, St Petersburg, FL, USA, and* [8]*Department of Geriatric Medicine, Kyorin University, School of Medicine, Mitaka, Japan*

doi:10.1111/j.1365-2567.2007.02781.x
Received 12 July 2007; revised 21 October 2007; accepted 9 November 2007.
Correspondence: T. Kizaki, PhD, Department of Molecular Predictive Medicine and Sport Science, Kyorin University, School of Medicine, 6-20-2, Shinkawa, Mitaka, Tokyo 181-8611, Japan.
Email: kizaki@kyorin-u.ac.jp
Senior author: Takako Kizaki, email: kizaki@kyorin-u.ac.jp

Summary

Toll-like receptors (TLRs) play an important role in innate immunity while, β_2-adrenergic receptors (β_2AR) provide the key linkages for the sympathetic nervous system to regulate the immune system. However, their role in macrophages remains uncertain. Here, we demonstrate the cross-talk between β_2AR and TLR signalling pathways. Expression of β_2AR was down-regulated by TLR4 ligand lipopolysaccharide (LPS) stimulation. To investigate the physiological consequence of this down-regulation RAW264 cells, a macrophage cell line, were transfected with a β_2AR expression vector (RAWar). Both LPS-stimulated inducible nitric oxide synthase (NOS II) expression and NO production were markedly suppressed in the RAWar cells. The activation of nuclear factor-κB (NF-κB) and degradation of the inhibitor of NF-κB (IκBα) in response to LPS were markedly decreased in these cells. The level of β-arrestin 2, which regulates β_2AR signalling, was also reduced in RAW264 cells after stimulation with LPS, but not in RAWar cells. Overexpression of β-arrestin 2 (RAWarr2) also inhibited NO production and NOS II expression. Furthermore, we demonstrated that β-arrestin 2 interacted with cytosolic IκBα and that the level of IκBα coimmunoprecipitated by anti-β-arrestin 2 antibodies was decreased in the RAW264 cells but not in RAWar or RAWarr2 cells. These findings suggest that LPS-stimulated signals suppress β_2AR expression, leading to down-regulation of β-arrestin 2 expression, which stabilizes cytosolic IκBα and inhibits the NF-κB activation essential for NOS II expression, probably to ensure rapid and sufficient production of NO in response to microbial attack.

Keywords: β_2-adrenergic receptor; monocytes/macrophages; nitric oxide; nuclear factor-κB; toll-like receptor

Introduction

The ability of the innate immune system to recognize and respond to microbial components has been chiefly attributed to a family of type I transmembrane receptors termed Toll-like receptors (TLRs) that are expressed abundantly on antigen-presenting cells such as macrophages and dendritic cells and can discriminate among the distinct molecular patterns associated with microbial components.[1,2] The TLR-initiated activation of nuclear factor-κB (NF-κB) is essential for the regulation of inducible nitric oxide synthase (NOS II) and several proinflammatory cytokines, which are produced in response to invading pathogens. The NO produced by NOS II has a number of important biological functions, including roles in host defence against intracellular pathogens and tumour-cell killing. Although this basic definition is still accepted, over the past decade NO has been shown to play a much more diverse role not only in the immune system but also in other organ systems, including both beneficial and detrimental effects.[3,4] For example, the systemic inflammatory response syndrome, which includes

severe septic shock and multiple organ system failure, remains a leading cause of death in critically ill patients. Therefore, it is necessary to clarify the molecular mechanisms of TLR-initiated signalling that lead to NO production in response to microbial components.

Nuclear factor-κB is found predominantly in the cytoplasm complexed with members of the inhibitor of NF-κB (IκB) family. The release of NF-κB from IκB proteins is an essential step in the generation of transcriptionally competent NF-κB. The consensus is that IκB proteins mask the nuclear localization signals of NF-κB proteins, thereby regulating NF-κB activity, primarily by limiting their nuclear translocation. Recent studies, however, have indicated that IκBα is detected in both the nucleus and cytoplasm and that although the NF-κB complexes shuttle between the nucleus and cytoplasm under all conditions, they are unable to bind DNA because of their association with proteins of the IκB family.[5–7] Nuclear IκBα is not sensitive to signal-induced degradation. Therefore, following stimulation, NF-κB activities are dependent on the level of cytoplasmic NF-κB/IκBα complexes.

Recently, we demonstrated that the level of β_2-adrenergic receptor (β_2AR) expression influences TLR4 signalling.[8] β_2AR is a member of a family of G protein-coupled receptors (GPCRs) and is the key link involved in immune system regulation via the sympathetic nervous system.[9,10] Primary and secondary lymphoid organs, such as the thymus, spleen and lymph nodes, receive extensive sympathetic/noradrenergic innervation, and lymphocytes, macrophages and many other immune cells bear functional β_2AR. Therefore, β_2AR stimulation regulates pro-inflammatory cytokine production, lymphocyte traffic and proliferation, and antibody secretion through cyclic adenosine monophosphate (cAMP) generation and protein kinase A (PKA) activation.[10,11] However, the role of β_2AR in the TLR signalling pathway in macrophages remains vague. On the other hand, arrestins are cytosolic proteins that play a critical role in the regulation of GPCR signalling.[12,13] Recent studies have shown that they also interact with their partner molecules in a variety of signalling pathways, including NF-κB signalling.[14–16] In the present study, we investigated the physiological consequence of the down-regulation of β_2AR expression in macrophages and analysed the cross-talk between the signalling of β_2AR and TLRs.

Materials and methods

Cell culture

The murine macrophage cell line RAW264 (RCB0535) was purchased from RIKEN Cell Bank (Ibaraki, Japan) and cultured as described in our previous study.[17] The cells were stimulated with 1 μg/ml lipopolysaccharide (LPS) from *Escherichia coli* 055 (Sigma-Aldrich, St Louis, MO). Cell viability was assessed using the trypan blue dye exclusion test and cell size was measured by flow cytometric analysis of forward light scatter characteristics using a FACSCalibur flow cytometer (Becton Dickinson, Mountain View, CA).

Electrophoretic mobility shift assay (EMSA)

Nuclear extracts were prepared as described elsewhere.[18] The NF-κB oligonucleotide probe (5′-AGT TGA GGG GAC TTT CCC AGG-3′) was purchased from Promega (Madison, WI) and labelled with biotin at its 3′ end. The nuclear protein (2 μg) and excess amounts of labelled oligonucleotide probes were incubated in 20 μl EMSA buffer [20 mM HEPES, pH 7·6, 10 mM $(NH_4)_2SO_4$, 1 mM dithiothreitol, 1 mM ethylenediaminetetraacetic acid (EDTA), 0·2% Tween, 30 mM KCl, 1 μg poly (dI-dC), 1 μg poly L-lysine] at room temperature for 15 min, electrophoresed in 7% polyacrylamide gels, transferred onto the Biodyne Plus Membane (Pall BioSupport Division, Port Washington, NY), and cross-linked in ultraviolet light. To detect signals, the blots were incubated with streptavidin–horseradish peroxidase conjugate in a blocking reagent for 15 min and with a chemiluminescent reagent for 5 min. The blots were then exposed to Kodak X Omat AR film (GE Healthcare Bio-Science, Piscataway, NJ).

Western blotting analysis

Cell membrane proteins were prepared using the Plasma Membrane Protein Extraction Kit (Bio Vision, Mountain View, CA). Cytoplasmic protein extracts were prepared as described previously (30). The protein concentration was determined using the Bradford reagent (BioRad, Hercules, CA), and equal amounts of membrane proteins or cytoplasmic proteins were loaded. The samples were separated by 10% sodium dodecyl sulphate–polyacrylamide gel electrophoresis (SDS–PAGE) and transferred on to polyvinylidene difluoride membranes (Applied Biosystems, Foster City, CA). The membranes were blocked with 10% non-fat dried milk in Tris-buffered saline and incubated with goat polyclonal antibodies against β_2AR, goat polyclonal antibodies against β-arrestin 2, or rabbit polyclonal antibodies against IκBα and NOS II (Santa Cruz Biotechnology, Santa Cruz, CA); this was followed by incubation with appropriate secondary antibodies (horseradish peroxidase-conjugated rabbit anti-goat or goat anti-rabbit immunoglobulin G; Dako, Kyoto, Japan). To ensure equal protein loading, the membranes were incubated with rabbit anti-actin or anti-glyceraldehyde-3-phosphate dehydrogenase (GAPDH) (Santa Cruz Biotechnology) for the detection of cytoplasmic or cell surface GAPDH[19] after stripping. Immunoreactivity was visualized using an enhanced chemiluminescence reagent (ECL; GE Healthcare Bio-Science).

Immunoprecipitation

The cells were lysed with lysis buffer (20 mM Tris–HCl, pH 7·6, 150 mM NaCl, 2 mM EDTA, 0·5% Nonidet P-40 and protease inhibitors). The samples were clarified by centrifugation at 21 000 ***g*** at 4° for 30 min. The protein concentration was determined using the Bradford reagent (Bio-Rad). β-Arrestin 2 was immunoprecipitated with anti-β-arrestin 2 monoclonal antibodies (Santa Cruz Biotechnology) from equal samples, followed by treatment with 10 μl protein G–Sepharose beads (GE Healthcare Bio-Science). After extensive washing, the complexes were analysed by SDS–PAGE and Western blotting by using rabbit polyclonal antibodies against IκBα.

Determination of nitrite concentration

Nitrite in the cell culture supernatants was measured using the assay system of Ding *et al.*[20] The nitrite concentration was calculated by comparison with sodium nitrite, which was used as a standard. In some experiments, 200 μM pyrrolidine dithiocarbamate (PDTC, Sigma) was added to the cultures.

Determination of intracellular cAMP concentration

Cells were cultured with or without LPS for 6 hr and were stimulated with Salbutamol (1×10^{-6} M) for the final 30 min. Cell supernatants were then removed and cells were lysed. Intracellular cAMP was determined with a commercially available enzyme immunoassay (GE Healthcare Bio-Science).

Real-time polymerase chain reaction (PCR)

Total cellular RNA was extracted from cells using the RNeasy Mini Kit (Qiagen, Hilden, Germany), and aliquots of 2 μg were reverse-transcribed with ReverScript I (Wako Pure Chemical Industries, Osaka, Japan) and an oligo-dT(15-mer) (Roche Diagnostics, Indianapolis, IN) at 42° for 50 min. The complementary DNAs (cDNAs) were amplified by PCR under the following conditions using the oligonucleotide primers and cycles listed in Table 1: 94° for 30 seconds, 55° for 30 seconds, and 72° for 30 seconds for NOS II and 18S ribosomal RNA (rRNA), and 94° for 30 seconds, 60° for 30 seconds, and 72° for 30 seconds for total and transfected β_2AR and β-arrestin 2. The quantity of the cDNA template included in these reactions and the number of amplification cycles were optimized to ensure that the reactions were stopped during the linear phase of product amplification, thus permitting semiquantitative comparisons of messenger RNA (mRNA) abundance between different RNA preparations.

β_2AR and β-arrestin 2 plasmid constructs and stable transfection

Full-length murine β_2AR (*$\beta_2$ar*) and β-arrestin 2 (*βarrestin2*) cDNAs were obtained by PCR using the primers 5′-GCTGAATGAAGCTTCCAGGA-3′ (sense) and 5′-GCCTGTATTACAGTGGCGAG-3′ (antisense) for β_2AR and 5′-GGCGGGCGGAGGGCGGCGAG-3′ (sense) and 5′-CGTCCTAGCAGAACTGGTCA-3′ (antisense) for β-arrestin 2. The amplified β_2AR and β-arrestin 2 fragments were subcloned into the pGEM-T Easy vector (Promega) and then into *Not*I-digested pcDNA4 (Invitrogen, Carlsbad, CA). The amplified PCR products were sequenced using an automatic DNA sequencer (Applied Biosystems). The plasmid DNA used for transfection was prepared using the EndoFree Plasmid Kit (Qiagen). RAW264 cells were transfected with the pcDNA4 vector, pcDNA4-$\beta_2$ar, or pcDNA4-βarrestin2 using LipofectAMINE Reagent (Invitrogen). Selection was initiated in a medium containing 500 μg/ml Zeocine (Invitrogen).

Luciferase assays

The full-length murine NOS II promoter fragment was cloned into the pGL3-enhancer luciferase reporter gene vector (Promega) (pGL3-NOS II) as described previously.[21] RAW264 cells were transfected using the LipofectAMINE Reagent with constructs containing the luciferase reporter gene, and luciferase activity was determined using the Dual Luciferase Assay System Kit (Promega) as described elsewhere.[21] Activity was normalized relative to an internal cotransfected constitutive control (*Renilla* luciferase expression vector, pRL-TK; Promega). In some

Table 1. Oligonucleotide sequences used for polymerase chain reaction

	Forward	Reverse	Cycle
β_2AR	GGAGCAGGATGGGCGGACGG	GCCTTCCATGCCTGGGGGAT	34
Transfected β_2AR	GGAGCAGGATGGGCGGACGG	TGGTGATGGTGATGATGACC	34
β-arrestin 2	GCAGCCAGGACCAGAGGACA	CCACGCTTCTCTCGGTTGTC	35
NOS II	CTTCCGAAGTTTCTGGCAGCAGCG	GAGCCTCGTGGCTTTGGGCTCCTC	26
18S	GAGAAACGGCTACCACATCC	CCCAAGATCCAACTACGAGC	26

β_2AR, β_2-adrenergic receptor; NOS II, nitric oxide synthase II.

experiments, RAW264 cells were transiently cotransfected with the NF-κB-responsive promoter reporter–luciferase construct pNF-κB-Luc (Clontech, Palo Alto, CA) or pGL3-NOS II and pcDNA4-$\beta_2$ar or IκBα dominant-negative vector pCMV-IκBαM (Clontech).

Statistical analysis

Student's *t*-test for unpaired samples was used to compare two means. For more than two groups, statistical significance of the data was assessed by analysis of variance. Where significant differences were found, individual comparisons were made between groups using the *t*-statistic and adjusting the critical value according to the Bonferroni method. Differences were considered significant at $P < 0{\cdot}05$. Data in the text and figures are expressed as means ± SEM.

Results

Preventing the down-regulation of β_2AR inhibits LPS-stimulated NOS II expression

Levels of both β_2AR protein and β_2AR mRNA were markedly decreased in RAW264 cells following LPS stimulation (Fig. 1a). To investigate the role of β_2AR down-regulation in response to LPS, a stable β_2AR transfectant (RAWar) and a vector control (RAWvec) were established. Although the levels of both β_2AR protein and mRNA expression were notably decreased in RAWvec cells following LPS stimulation, the down-regulation of β_2AR expression was prevented in the RAWar cells (Fig. 1b). The transfected β_2AR protein did not have a tag sequence capable of modifying β_2AR function so the protein levels of only transfected β_2AR could not be analysed. The mRNA levels of transfected β_2AR were low in unstimulated RAWar cells but markedly increased in the cells following LPS stimulation (Fig. 1c). In our previous study, we showed that the levels of both protein and mRNA of transfected cDNA cloned into the pcDNA4 vector were low in unstimulated RAW264 cells but were markedly increased in the cells following LPS stimulation.[17] Therefore, it appears that total β_2AR expression in unstimulated RAWar cells was not much higher than in RAWvec cells and that the decrease in intrinsic β_2AR expression in the LPS-stimulated RAWar cells was masked by the increased expression of transfected β_2AR as the result of the LPS stimulation. Although, the intracellular cAMP concentration in RAWar cells stimulated with salbutamol was similar to that in RAWvec cells, LPS

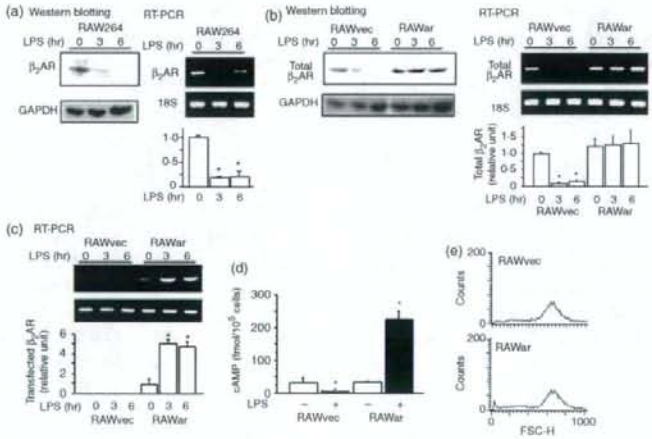

Figure 1. Lipopolysaccharide (LPS) stimulation down-regulates β_2-adrenergic receptor (β_2AR) expression. (a) RAW264 cells were stimulated with LPS. The protein levels of β_2AR and GAPDH (loading control) in the plasma membrane were analysed by Western blotting (left panel). The β_2AR messenger RNA (mRNA) and 18S ribosomal RNA (rRNA; loading control) were analysed by reverse transcription–polymerase chain reaction (RT-PCR; right upper panel). Bar graphs show the relative intensity of the PCR bands from three separate experiments (mean ± SEM) (right lower panel). *$P < 0{\cdot}01$ versus 0 hr. (b) RAW264 cells were transfected with the β_2ar construct or vector alone. The protein levels of β_2AR and GAPDH (left panel) and mRNA expressions of β_2AR and 18S rRNA (right upper panel) were analysed as in (a). Bar graphs show the relative intensities of the PCR bands from three separate experiments (mean ± SEM) (right lower panel). *$P < 0{\cdot}01$ versus 0 hr. (c) mRNA expressions of β_2AR and 18S rRNA (upper panel) were analysed as in (a). Bar graphs show the relative intensities of the PCR bands from three separate experiments (mean ± SEM) (lower panel). *$P < 0{\cdot}01$ versus 0 hr. (d) Cells were cultured with or without LPS for 6 hr and were stimulated with salbutamol (1×10^{-6} M) for the final 30 min. Then, intracellular cyclic AMP concentrations were analysed. *$P < 0{\cdot}05$ versus without LPS. (e) Cell size was measured by flow cytometric analysis of forward light scatter characteristics (FSC).

stimulation decreased the accumulation of intracellular cAMP in RAWvec cells but increased it in RAWar cells (Fig. 1d), suggesting that the transfected β_2AR was functionally active. Similar histograms of the distribution of forward light scatter characteristics were observed in RAWvec and RAWar cells, suggesting that the β_2AR transfection did not alter the cell size (Fig. 1e). In addition, cell viabilities were more than 98% in both cells.

The effects of forced β_2AR expression on NO production were examined. The nitrite concentration in the culture supernatants of the LPS-stimulated RAWar cells was considerably lower than in the culture supernatants of the RAWvec cells (Fig. 2a). After stimulation with LPS for 6 hr, a distinct 130 000 molecular weight NOS II protein band was observed in the RAWvec cells but not in the RAWar cells (Fig. 2b). Although a protein band corresponding to NOS II was observed in the RAWar cells after stimulation with LPS for 24 hr, the expression level was apparently lower than in the RAWvec cells. Similar results were obtained on reverse transcription PCR analysis of NOS II mRNA expression (Fig. 2b).

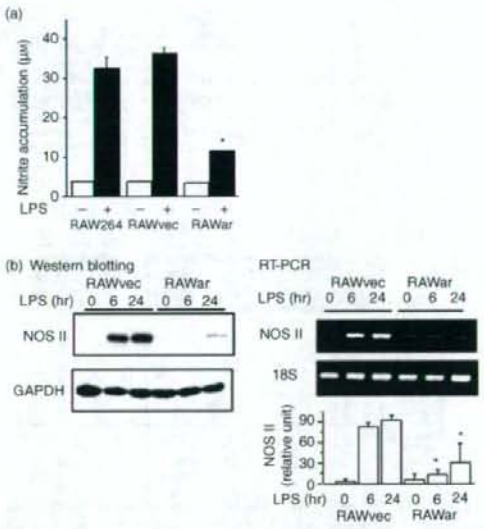

Figure 2. Forced β_2-adenergic receptor (β_2AR) expression suppresses nitric oxide (NO) production and nitric oxide synthase II (NOS II) expression. (a) Cells were stimulated with lipopolysaccharide (LPS) for 24 hr, and nitrite accumulation in the supernatants was measured using the Griess reagent. The results are expressed as means ± SEM from three-well cultures. *$P < 0{\cdot}001$ versus LPS-stimulated RAW264 or RAWvec cells. (b) The protein levels of NOS II and GAPDH (left panel) and messenger RNA expressions of NOS II and 18S ribosomal RNA were analysed as in A (right upper panel). Bar graphs show the relative intensity of the polymerase chain reaction bands from four separate experiments (mean ± SEM) (right lower panel). *$P < 0{\cdot}01$ versus corresponding RAWvec cells. Data shown are representative of three or four separate experiments.

Preventing the down-regulation of β_2AR inhibits LPS-stimulated NF-κB activation.

Next, the effects of forced β_2AR expression on NF-κB activation in response to LPS were analysed. As illustrated in Fig. 3(a), marked NF-κB activation was observed in the RAWvec cells stimulated with LPS for 3 and 6 hr but not in the RAWar cells. The level of cytoplasmic IκBα was decreased in the RAWvec cells after LPS stimulation for 6 hr but this level was not decreased in the RAWar cells (Fig. 3b). To further confirm the role of β_2AR in LPS-stimulated NF-κB activation, the effects of forced β_2AR expression on NF-κB-dependent gene transcription were analysed. NF-κB-mediated-luciferase reporter activity (Fig. 3c) and NOS II promoter activity (Fig. 3d) after stimulation with LPS were inhibited in cells that were cotransfected with the pcDNA4-$\beta_2$ar construct (AR) as well as in cells cotransfected with pCMV-IκBαM (DN-κB). These findings suggested that β_2AR functions as a negative regulator of NF-κB activation by inhibiting IκBα degradation in LPS-stimulated macrophages. Previously, it has been shown that PDTC blocks NF-κB activation by inhibiting IκBα degradation and subsequently the translocation of NF-κB subunits to the nucleus.[22] To elucidate the effects of NF-κB activation on the expression of the responsive gene, *Nos2*, PDTC was added to the RAW264 cell cultures at several time-points after the addition of LPS, and accumulation of NO in the supernatants was analysed after LPS stimulation for 24 hr. As illustrated in Fig. 3(e), when PDTC was added to cultures at 0–9 hr after the addition of LPS, the NO concentrations in these cultures were markedly lower than those in cultures stimulated with LPS for 24 hr without PDTC (right column), indicating that continuous NF-κB activation is essential for adequate NOS II induction.

β_2AR regulates NF-κB activation through β-arrestins

As β-arrestin 2 has been reported to interact with IκBα,[15,16] we examined whether β-arrestin 2 participates in the β_2AR-mediated regulation of IκBα degradation and NF-κB activation in response to LPS. The expression of β-arrestin 2 was also down-regulated in the LPS-stimulated RAW264 cells (Fig. 4, left panels). Forced β_2AR expression abolished the down-regulation of β-arrestin 2 expression (middle panels), suggesting that β-arrestin 2 expression was regulated by β_2AR. Deletion of β_2AR by small interfering RNA (siRNA) decreased β-arrestin 2 expression (data not shown), supporting the theory that β-arrestin 2 expression is regulated by β_2AR. To investigate the role of β-arrestin 2 down-regulation in response to LPS, a stable β-arrestin 2 transfectant (RAWarr2) was

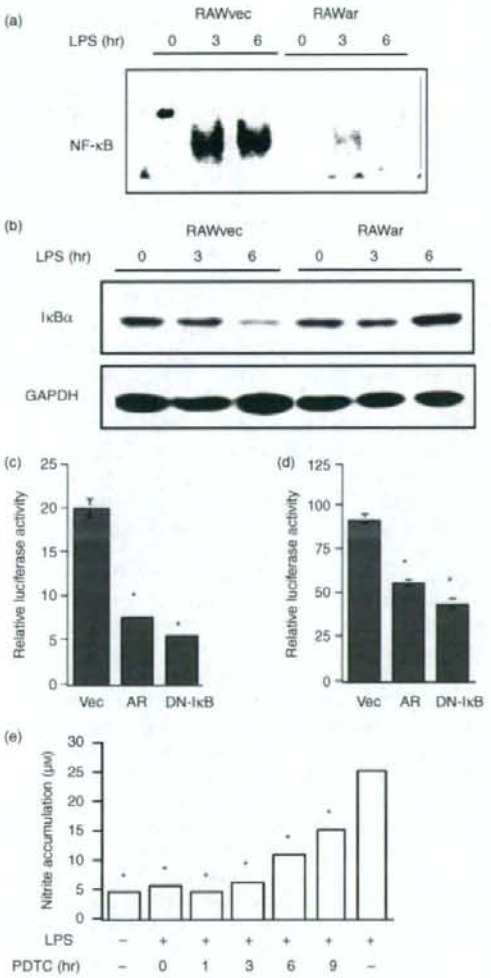

established (Fig. 4, right panels). Since transfection with the vector did not influence NO production (Fig. 1c), cells transfected with β-arrestin 2 were compared with RAW264 cells. As shown in the RAWar cells (Fig. 2), NO production (Fig. 5a) and NOS II protein and mRNA expressions (Fig. 5b) were definitely decreased in the RAWarr2 cells.

Anti-β-arrestin 2 antibodies coimmunoprecipitated IκBα in RAW264 cells before, but not after, LPS stimulation for 6 hr (Fig. 6). On the other hand, the amount of IκBα coprecipitated by anti-β-arrestin 2 antibodies was not reduced but rather was increased in the RAWar and RAWarr2 cells after LPS stimulation, indicating that the LPS-stimulated down-regulation of β_2AR and β-arrestin 2 is essential for IκBα degradation.

Figure 3. Forced β_2-adrenergic receptor (β_2AR) expression suppresses nuclear factor-κB (NF-κB) activation. (a) The vector control cells and β_2AR transfectant were stimulated with lipopolysaccharide (LPS), and NF-κB activation was analysed by electrophoretic mobility shift assay. (b) The vector control cells and β_2AR transfectant were stimulated with LPS, and cytoplasmic inhibitor of NF-κB (IκBα) and GAPDH (loading control) were analysed by Western blotting. (c, d) RAW264 cells were cotransfected with the pNF-κB-Luc vector (c) or the NOS II promoter–luciferase construct (d) and vector (Vec), pcDNA4-β_2AR (AR) or pCMV-IκBαM (DN-IκB). The cells were cultured with LPS for 24 hr, and luciferase activities were determined. The results are expressed as means ± SEM from six-well cultures. $^*P < 0{\cdot}001$ versus cells cotransfected with Vec. (e) Pyrrolidine dithiocarbamate (PDTC) was added to the cultures at the indicated time-points after addition of LPS. Nitrite accumulation in the supernatants at 24 hr of culture was measured using the Griess reagent. The results are expressed as means ± SEM from three-well cultures. The error bars are too small to be distinguishable in the figure (numeric data from the left bar: 3·75 ± 0·18, 5·07 ± 0·22, 4·22 ± 0·07, 5·69 ± 0·12, 10·38 ± 0·06, 15·00 ± 0·05, and 25·20 ± 0·28). $^*P < 0{\cdot}001$ versus LPS-stimulated cells without PDTC. Data shown are representative of two or three separate experiments.

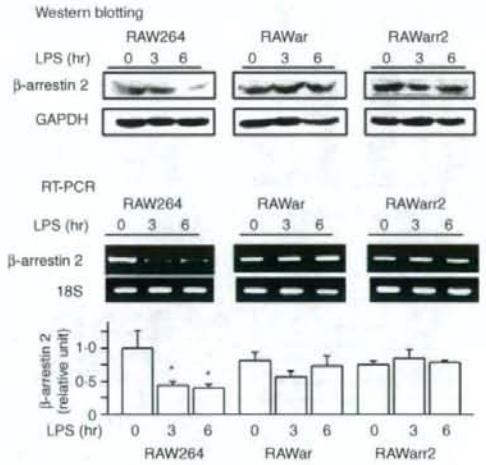

Figure 4. Lipopolysaccharide (LPS) stimulation down-regulates β-arrestin 2 expression. RAW264, RAWar, and RAWarr2 cells were stimulated with LPS, and the protein levels of β-arrestin 2 and GAPDH (upper panel) and messenger RNA expressions of β-arrestin 2 and 18S ribosomal RNA (middle panel) were analysed as in Fig. 1(a). Bar graphs show the relative intensity of the band from three separate experiments (mean ± SEM) (lower panel). $^*P < 0{\cdot}01$ versus 0 hr.

Discussion

In this study, we investigated the role played by β_2AR in the antimicrobial responses of macrophages. First, we demonstrated that β_2AR expression is decreased by LPS

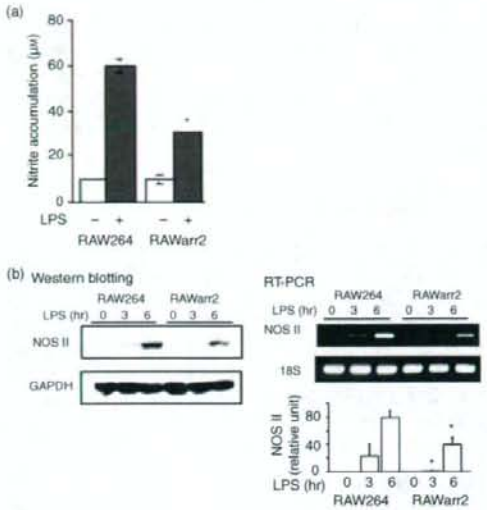

Figure 5. Forced β-arrestin 2 expression suppresses nitric oxide (NO) production and nitric oxide synthase II (NOS II) expression. (a) Cells were stimulated with lipopolysaccharide (LPS) for 24 hr, and nitrite accumulation in the supernatants was measured using the Griess reagent. The results are expressed as means ± SEM from three-well cultures. $^*P < 0{\cdot}001$ versus LPS-stimulated RAW264 cells. (b) The protein levels of NOS II and GAPDH (left panel) and messenger RNA expressions of NOS II and 18S ribosomal RNA (light upper panel) were analysed as in Fig. 1(a). Bar graphs show the relative intensity of the polymerase chain reaction bands from three separate experiments (mean ± SEM) (right lower panel). $^*P < 0{\cdot}01$ versus corresponding RAW264 cells. Data shown are representative of three to four separate experiments.

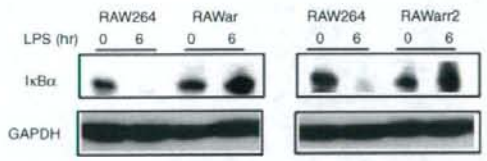

Figure 6. β-arrestin 2 interacts with cytosolic inhibitor of NF-κB (IκBα). Before and after stimulation with lipopolysaccharide (LPS) for 6 hr, cells were lysed and immunoprecipitated with anti-β-arrestin 2 antibodies. Western blotting analysis was performed using anti-IκBα antibodies (upper panel). The protein levels of GAPDH in equal amounts of lysates were used for control (lower panel).

stimulation. To investigate the role of β_2AR down-regulation in response to LPS directly, we established a macrophage cell line, RAWar. Prevention of the down-regulation of β_2AR expression in RAWar cells resulted in reduced NO production, suggesting that the LPS-associated down-regulation of β_2AR expression plays an important role in NO production in macrophages.

Decreases in NOS II mRNA expression were observed in the RAWar cells, indicating that NOS II expression was transcriptionally down-regulated by forced β_2AR expression. Prevention of the down-regulation of β_2AR expression in the RAWar cells resulted in a marked decrease in NF-κB activation and inhibited cytosolic IκBα degradation, indicating that the forced β_2AR expression inhibited LPS-induced NF-κB activation by IκBα stabilization.

On the other hand, β-arrestins, which are universally expressed members of the arrestin family, are the major regulators of GPCR signalling and bind to activated GPCRs, causing receptor desensitization and internalization.[14] Recently, β-arrestins have been shown to play functional roles in the regulation of a variety of signalling pathways and in the mediation of cross-talk between signalling pathways. Moreover, there is accumulating evidence that β-arrestin 2, which is expressed abundantly in the spleen, is functionally involved in some important immune responses.[23–26] We have demonstrated that β-arrestin 2 is down-regulated in LPS-stimulated RAW264 cells. Down-regulation of β-arrestin 2 was abolished in RAWar cells, suggesting that β-arrestin 2 expression is regulated by β_2AR. These findings suggest that β_2AR participates in signal transduction pathways from TLR4 by regulating the level of β-arrestin 2 expression. Meanwhile, the amount of IκBα coimmunoprecipitated by anti-β-arrestin 2 antibodies was decreased in the RAW264 cells after their stimulation with LPS but not in the RAWar or RAWarr2 cells, suggesting that β_2AR inhibited LPS-induced NF-κB activation by stabilizing IκBα through β-arrestin 2. The release of NF-κB following the degradation of IκBα proteins is an essential step in the generation of transcriptionally competent NF-κB. In addition, NF-κB activity following stimulation is dependent on the level of cytoplasmic NF-κB/IκBα complexes free from stabilizing factors. Therefore, the following appear likely: (1) LPS-stimulated signals suppress β_2AR expression, (2) the reduction of β_2AR results in the down-regulation of β-arrestin 2 expression, (3) β-arrestin 2 stabilizes cytoplasmic IκBα and inhibits NF-κB activation (so reduction in the level of β-arrestin 2 accelerates IκBα degradation and NF-κB activation in LPS-stimulated cells) and (4) nuclear translocation of NF-κB enhances NOS II expression.

The cross-talk between β_2AR and the TLR signalling pathways is schematically summarized in Fig. 7.

Catecholamines increase cAMP via β_2AR activation, and PKA activation inhibits NF-κB-induced transcription by phosphorylating cAMP responsive element binding protein (CREB), which competes with p65 for the limited amounts of CREB-binding protein (CBP) (Fig. 7a(ii)).[27] However, β_2AR agonists did not suppress NO production (unpublished observation). In the present study, we demonstrated that LPS stimulation suppressed the cAMP accumulation in RAWvec cells stimulated with a β_2AR

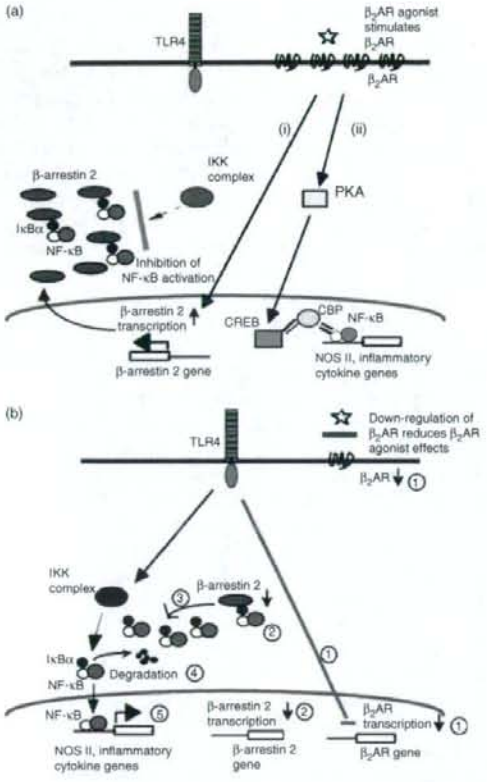

Figure 7. Cross-talk between β_2-adrenergic receptor (β_2AR) and Toll-like receptor (TLR) signalling pathways. (a) β_2AR agonists suppress nuclear factor-κB (NF-κB) activation by increasing cytoplasmic β-arrestin 2, which stabilizes the NF-κB/inhibitor of NF-κB (IκBα) complexes in cytoplasm (i) or by activating cAMP response element binding protein (CREB), which then produces competition between CREB-binding protein (CBP) and NF-κB in the nucleus (ii). (b) TLR4-dependent signals lead to the following steps both in the presence or absence of β_2AR agonists: ① TLR4-dependent down-regulation of β_2AR expression, ② down-regulation of β-arrestin 2, ③ release of NF-κB/IκBα complexes in the cytoplasm, ④ degradation of IκBα, and ⑤ translocation of NF-κB to the nucleus and transcription of its target genes.

agonist. In addition, we showed that prevention of the down-regulation of β_2AR inhibits the degradation of IκBα through β-arrestin 2, which stabilizes IκBα in the steady state (Fig. 7a(ii)). Therefore, the down-regulation of expression of both β_2AR and β-arrestin 2 by the TLR4-dependent pathway might provide a mechanism for 'escaping' anti-proinflammatory signals, such as the β_2AR–cAMP–PKA pathway[27] or the β_2AR–β-arrestin 2–IκBα pathway. As the levels of β_2AR ligands vary under different conditions, understanding the cross-talk between TLRs and β_2AR pathways may have both physiological and pathophysiological importance. Taken together, the observations of the present study regarding the regulation of TLR4 signalling through β_2AR appear to provide another therapeutic target for the regulation of inflammatory disease conditions.

Acknowledgements

We thank Dr T. Seya (Hokkaido University, Sapporo, Japan) for providing helpful comments. This study was supported in part by Grants-in-Aid for Scientific Research (including the Academic Frontier Project) from the Japanese Ministry of Education, Culture, Sports, Science and Technology and by a Grant-in-Aid for Promotion and Mutual Aid Corporation for Private Schools of Japan (to T.K. and H.O.).

References

1 Takeda K, Kaisho T, Akira S. Toll-like receptors. *Annu Rev Immunol* 2003; **21**:335–76.
2 Janeway CA Jr, Medzhitov R. Innate immune recognition. *Annu Rev Immunol* 2002; **20**:197–216.
3 Hierholzer C, Harbrecht B, Menezes JM *et al.* Essential role of induced nitric oxide in the initiation of the inflammatory response after hemorrhagic shock. *J Exp Med* 1998; **187**:917–28.
4 Bogdan C. Nitric oxide and the immune response. *Nat Immunol* 2001; **2**:907–16.
5 Lain de Lera T, Folgueira L, Martin AG *et al.* Expression of IkappaBalpha in the nucleus of human peripheral blood T lymphocytes. *Oncogene* 1999; **18**:1581–8.
6 Tergaonkar V, Correa RG, Ikawa M, Verma IM. Distinct roles of IkappaB proteins in regulating constitutive NF-kappaB activity. *Nat Cell Biol* 2005; **7**:921–3.
7 Rodriguez MS, Thompson J, Hay RT, Dargemont C. Nuclear retention of IkappaBalpha protects it from signal-induced degradation and inhibits nuclear factor kappaB transcriptional activation. *J Biol Chem* 1999; **274**:9108–15.
8 Itoh CE, Kizaki T, Hitomi Y *et al.* Down-regulation of beta2-adrenergic receptor expression by exercise training increases IL-12 production by macrophages following LPS stimulation. *Biochem Biophys Res Commun* 2004; **322**:979–84.
9 Downing JE, Miyan JA. Neural immunoregulation: emerging roles for nerves in immune homeostasis and disease. *Immunol Today* 2000; **21**:281–9.
10 Elenkov IJ, Wilder RL, Chrousos GP, Vizi ES. The sympathetic nerve – an integrative interface between two supersystems: the brain and the immune system. *Pharmacol Rev* 2000; **52**:595–638.
11 Kohm AP, Sanders VM. Norepinephrine and beta 2-adrenergic receptor stimulation regulate CD4$^+$ T and B lymphocyte function *in vitro* and *in vivo*. *Pharmacol Rev* 2001; **53**:487–525.
12 Ferguson SS, Downey WE 3rd, Colapietro AM, Barak LS, Menard L, Caron MG. Role of beta-arrestin in mediating agonist-promoted G protein-coupled receptor internalization. *Science* 1996; **271**:363–6.

13 Ogasawara J, Sanpei M, Rahman N, Sakurai T, Kizaki T, Hitomi Y, Ohno H, Izawa T. β-adrenergic receptor trafficking by exercise in rat adipocytes: roles of G-protein-coupled receptor kinase-2, β-arrestin-2, and the ubiquitin–proteasome pathway. *FASEB J* 2006; **20**:350–2.

14 Luttrell LM, Lefkowitz RJ. The role of β-arrestins in the termination and transduction of G-protein-coupled receptor signals. *J Cell Sci* 2002; **115**:455–65.

15 Witherow DS, Garrison TR, Miller WE, Lefkowitz RJ. β-arrestin inhibits NF-κB activity by means of its interaction with the NF-κB inhibitor IκBα. *Proc Natl Acad Sci U S A* 2004; **101**:8603–7.

16 Gao H, Sun Y, Wu Y, Luan B, Wang Y, Qu B, Pei G. Identification of β-arrestin2 as a G protein-coupled receptor-stimulated regulator of NF-κB pathways. *Mol Cell* 2004; **14**: 303–17.

17 Kizaki T, Suzuki K, Hitomi Y *et al.* Uncoupling protein 2 plays an important role in nitric oxide production of lipopolysaccharide-stimulated macrophages. *Proc Natl Acad Sci U S A* 2002; **99**:9392–7.

18 Kizaki T, Ookawara T, Iwabuchi K *et al.* Age-associated increase of basal corticosterone levels decreases $ED2^{high}$, $NF\text{-}\kappa B^{high}$ activated macrophages. *J Leukoc Biol* 2000; **68**:21–30.

19 Raje CI, Kumar S, Harle A, Nanda JS, Raje M. The macrophage cell surface glyceraldehyde-3-phosphate dehydrogenase is a novel transferrin receptor. *J Biol Chem* 2007; **282**:3252–61.

20 Ding AH, Nathan CF, Stuehr DJ. Release of reactive nitrogen intermediates and reactive oxygen intermediates from mouse peritoneal macrophages. comparison of activating cytokines and evidence for independent production. *J Immunol* 1988; **141**:2407–12.

21 Kizaki T, Suzuki K, Hitomi Y *et al.* Negative regulation of LPS-stimulated expression of inducible nitric oxide synthase by AP-1 in macrophage cell line J774A.1. *Biochem Biophys Res Commun* 2001; **289**:1031–8.

22 Staal FJ, Roederer M, Herzenberg LA, Herzenberg LA. Intracellular thiols regulate activation of nuclear factor κB and transcription of human immunodeficiency virus. *Proc Natl Acad Sci U S A* 1990; **87**:9943–7.

23 Sun Y, Cheng Z, Ma L, Pei G. β-arrestin2 is critically involved in CXCR4-mediated chemotaxis, and this is mediated by its enhancement of p38 MAPK activation. *J Biol Chem* 2002; **277**:49212–9.

24 Barlic J, Andrews JD, Kelvin AA *et al.* Regulation of tyrosine kinase activation and granule release through β-arrestin by CXCR1. *Nat Immunol* 2000; **1**:227–33.

25 Fong AM, Premont RT, Richardson RM, Yu YR, Lefkowitz RJ, Patel DD. Defective lymphocyte chemotaxis in β-arrestin2- and GRK6-deficient mice. *Proc Natl Acad Sci U S A* 2002; **99**:7478–83.

26 Walker JK, Fong AM, Lawson BL, Savov JD, Patel DD, Schwartz DA, Lefkowitz RJ. β-arrestin-2 regulates the development of allergic asthma. *J Clin Invest* 2003; **112**:566–74.

27 Parry GC, Mackman N. Role of cyclic AMP response element-binding protein in cyclic AMP inhibition of NF-κB-mediated transcription. *J Immunol* 1997; **159**:5450–6.

Journal of proteome research

Article

Glycomic Analysis of Alpha-Fetoprotein L3 in Hepatoma Cell Lines and Hepatocellular Carcinoma Patients

Takatoshi Nakagawa, Eiji Miyoshi, Takayuki Yakushijin, Naoki Hiramatsu, Takumi Igura, Norio Hayashi, Naoyuki Taniguchi, and Akihiro Kondo

J. Proteome Res., **2008**, 7 (6), 2222-2233• DOI: 10.1021/pr700841q • Publication Date (Web): 15 May 2008

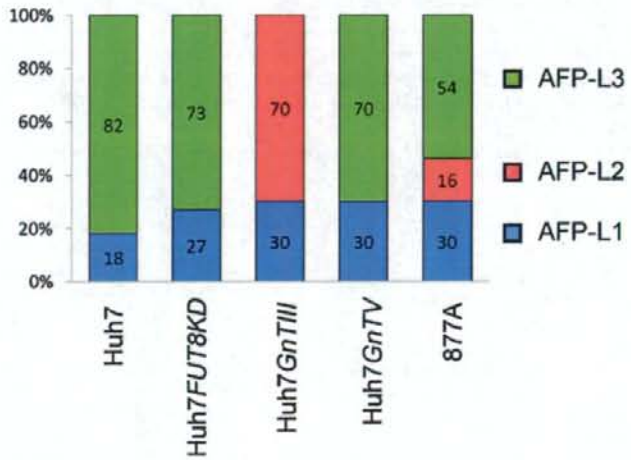

More About This Article

Additional resources and features associated with this article are available within the HTML version:

- Supporting Information
- Links to the 1 articles that cite this article, as of the time of this article download
- Access to high resolution figures
- Links to articles and content related to this article
- Copyright permission to reproduce figures and/or text from this article

View the Full Text HTML